

Novel Role of the Small GTPase Rheb: Its Implication in Endocytic Pathway Independent of the Activation of Mammalian Target of Rapamycin

Kota Saito, Yasuhiro Araki, Kenji Kontani, Hiroshi Nishina and Toshiaki Katada*

Department of Physiological Chemistry, Graduate School of Pharmaceutical Sciences, University of Tokyo, 7-3-1 Hongo, Bunkyo-ku, Tokyo 113-0033

Received January 8, 2005; accepted February 1, 2005

The Ras-homologous GTPase Rheb that is conserved from yeast to human appears to be involved not only in cell growth but also in nutrient uptake. Recent biochemical analysis revealed that tuberous sclerosis complex (TSC), a GTPase-activating protein (GAP), deactivates Rheb and that phosphatidylinositol 3'-kinase (PI3k)-Akt/PKB kinase pathway activates Rheb through inhibition of the GAP-mediated deactivation. Although mammalian target of rapamycin (mTOR) kinase is implicated in the downstream target of Rheb, the direct effector(s) and exact functions of Rheb have not been fully elucidated. Here we identified that Rheb expression in cultured cells induces the formation of large cytoplasmic vacuoles, which are characterized as late endocytic (late endosome- and lysosome-like) components. The vacuole formation required the GTP form of Rheb, but not the activation of the downstream mTOR kinase. These results suggest that Rheb regulates endocytic trafficking pathway independent of the previously identified mTOR pathway. The physiological roles of the two Rheb-dependent signaling pathways are discussed in terms of nutrient uptake and cell growth or cell cycle progression.

Key words: late endosome, lysosome, mTOR, Rheb, small GTPase.

Abbreviations: DMEM, Dulbecco's modified Eagle's minimum essential medium; GAP, GTPase-activating protein; mTOR, mammalian target of rapamycin; PI3k, phosphatidylinositol 3'-kinase; Rheb, *ras* homologue enriched in brain; TSC, tuberous sclerosis complex.

Members of the small GTPase Ras superfamily act as molecular switches that regulate a wide range of cellular functions including cell proliferation and differentiation. Ras homologue enriched in brain, Rheb, is a member of an atypical family of Ras-related G proteins, of which sequences in the GTP-binding domain have not been conserved (1). Di-Ras1, Di-Ras2, and ARHI also belong to the atypical GTPase family (2). Rheb was initially identified as a gene whose mRNA expression is increased in rat brain by seizures or by the stimulation of long-term potentiation (3). Recently, Rheb has received significant attention, since it was identified as a positive regulator of the mammalian target of rapamycin (mTOR) pathway, which regulates cell growth in response to various growth factors, cellular energy and nutrient levels (4–10). Moreover, the TSC1/TSC2 complex, of which mutations leads to tuberous sclerosis complex (TSC), was found to be a GTPase-activating protein (GAP) for Rheb (5–8, 11).

From recent biochemical studies in mammalian cells, Rheb-related signaling pathways leading to cell growth may be summarized as follows. The stimulation of growth factor receptors at the cell surface results in the activation of phosphatidylinositol 3'-kinase (PI3k), which then phosphorylates Akt/PKB (12, 13). The activated Akt

phosphorylates TSC2 to negatively regulate its GAP activity toward Rheb (6, 14, 15). This results in the accumulation of GTP-Rheb and stimulates the mTOR kinase activity (4–10). Phosphorylation of p70 ribosomal S6 kinase (S6K) and the translation initiation factor 4E-BP1, which are responsible for the increase in protein synthesis, has been implicated in the downstream events of mTOR kinase (16, 17). Thus, Rheb is involved in the signaling pathways responsible for cell growth and cell cycle progression.

On the other hand, Rheb appears to play an important role in intracellular uptake of nutrients such as amino acids. Rheb is conserved from yeast to human, and recent genetic studies have contributed significantly to the understanding of its function. In yeast, arginine uptake was regulated positively and negatively by TSC and Rheb, respectively (18–20). In addition, Tsc1 and Tsc2 knockouts in *Schizosaccharomyces pombe* exhibited abnormal intracellular distribution of an amino-acid permease (21). In human, TSC patients suffer from seizures and epilepsy, which may be related to the dysfunction of extracellular glutamate uptake in glial cells. The accumulated glutamate in the synaptic cleft may cause neuronal cell death. However, the linkage between Rheb activation and nutrient uptake and the molecular mechanism underlying TSC epileptogenesis have not been fully clarified.

In the present study, we found that Rheb activation induces the formation of large vacuoles in the cytoplasm

*To whom correspondence may be addressed. Tel: +81-3-5841-4750, Fax: +81-3-5841-4751, E-mail: katada@mol.f.u-tokyo.ac.jp

of Rheb-transfected cells, and that the vacuoles are characterized as late endosome- or lysosome-like organelles. The large vacuole formation was dependent on the GTPase cycle of Rheb and suppressed by inhibition of the PI3k activity. However, inhibition of mTOR kinase did not affect the Rheb-induced vacuole formation. These results suggest that Rheb plays an important role in endocytic trafficking pathway independent of the previously identified mTOR pathway that leads to cell growth and cell-cycle progression. Possible roles of Rheb are discussed in terms of the relationship between the Rheb-dependent endocytic pathway and nutrient uptake.

MATERIALS AND METHODS

Northern Blot Analysis—Expression patterns of Rheb and Rheb2 mRNAs were analyzed using human multiple tissue membranes (BD Biosciences). Full-length sequences of Rheb and Rheb2 that had been radiolabeled with [α - 32 P]dCTP were hybridized to the membranes overnight at 65°C in the Expresshyb solution (BD Biosciences), and the membranes were subjected to autoradiography (22).

Cell Culture and Transfection—MDCK, HeLa, 1321N1, and 293 cells were maintained in Dulbecco's modified Eagle's minimum essential medium (DMEM) supplemented with 10% fetal bovine serum. The cells cultured in a 35-mm dish were transfected with 1 μ g of DNA and 2 μ l of LipofectAMINE 2000 (Invitrogen) in Opti-MEM according to the manufacturer's protocol and incubated at 37°C for 16 h unless otherwise specified.

Confocal Microscopic Analysis—The transfected cells in a glass-based dish (35-mm diameter, Matsunami) were analyzed by Carl Zeiss confocal microscopy with LSM510 (23). For the analysis of dextran uptake and the labeling of acidic organelles (see Fig. 4), the transfected MDCK cells were further incubated at 37°C with 1 mg/ml of FITC-dextran (Molecular Probes) for 12 h (Fig. 4A) and 50 nM LysoTracker Green (Molecular Probes) for 1 h (Fig. 4B), then washed for four times with PBS before the confocal microscopic analysis. In some experiments (see Fig. 4C), MDCK cells were first incubated with 1 mg/ml of FITC-dextran in DMEM at 37°C for 4 h and further cultured without the dextran for an additional 20 h. The dextran-preloaded cells were transfected with Dsred-Rheb and incubated for the indicated times before the confocal microscopic analysis.

Analysis of Akt Kinase Activity—293 cells cultured in a 6-cm dish were transfected with 1.5 μ g of Myc-Akt and 1.5 μ g of FLAG or FLAG-Rheb and further incubated in the presence or absence of 50 μ M LY294002 (Calbiochem) for 16 h. The cells were solubilized with an extraction buffer consisting of 40 mM Na-Hepes (pH 7.4), 75 mM NaCl, 1% Triton X-100, 1 mM EDTA, 15 mM NaF, 1 mM Na_3VO_4 , 10 mM $\text{Na}_4\text{P}_2\text{O}_7$, 1 μ g/ml leupeptin, and 2 μ g/ml aprotinin, and the cell lysate was immunoprecipitated with Myc-antibody (Sigma) conjugated to Protein G-agarose (Amersham Biosciences). The immunocomplexes were washed three times with a buffer consisting of 50 mM Na-Hepes, 100 mM NaCl, 0.2% Triton X-100, 15 mM NaF, 1 mM Na_3VO_4 , 10 mM $\text{Na}_4\text{P}_2\text{O}_7$, 4 mM EDTA, 1 mM DTT, and 2 μ g/ml aprotinin, then twice with a kinase

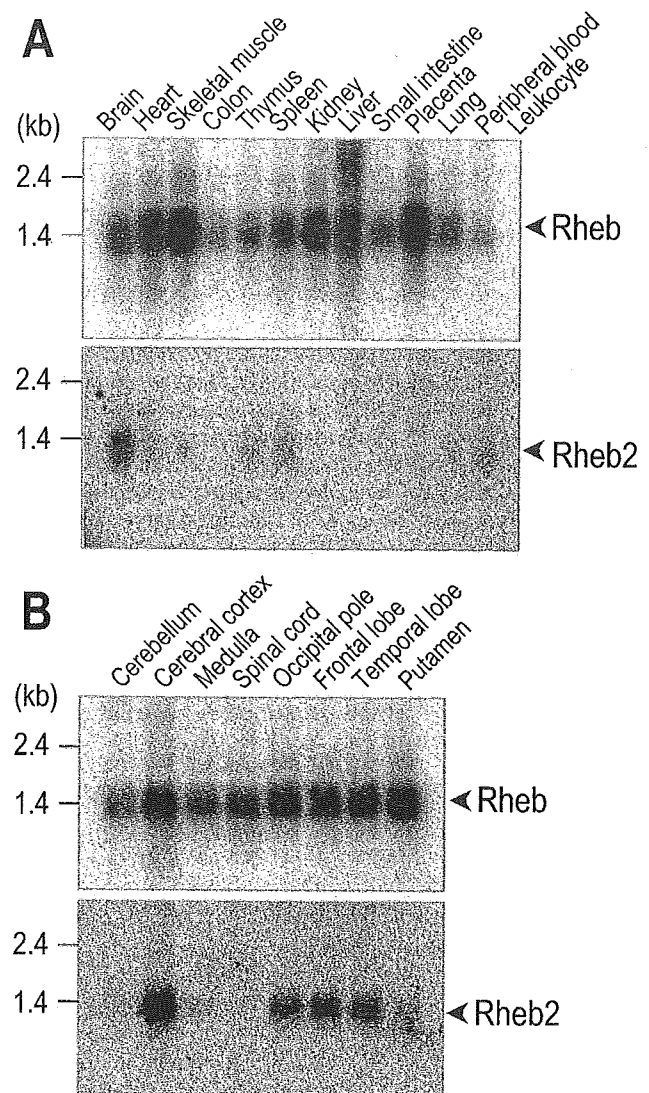


Fig. 1. Northern blot analysis of Rheb and Rheb2. Membranes blotted with RNAs obtained from various human tissues (A) and the brain regions (B) were hybridized with 32 P-labeled Rheb (top panels) and Rheb2 (bottom panels) probes, respectively, as described under "MATERIALS AND METHODS."

buffer consisting of 50 mM Na-Hepes, 0.01% Triton X-100, 1 mM DTT, 10 mM MgCl_2 . They were then incubated with the kinase buffer further supplemented with 50 μ M ATP, 3 μ Ci [γ - 32 P]ATP, and 10 μ g/ml of GST-GSK3 β at 37°C for 20 min. Phosphorylated proteins were analyzed by SDS-PAGE, and the radioactivity was visualized with a BAS-1800 bioimaging analyzer (Fuji Firm).

Analysis of mTOR Kinase Activity—293 cells in a 6-cm dish were transfected with 1.5 μ g of HA-S6K and 1.5 μ g of FLAG or FLAG-Rheb and further incubated in the presence or absence of 40 nM rapamycin (Calbiochem) for 5 h. The cells were washed with PBS and further cultured in DMEM supplemented with 0.1% BSA in the presence or absence of rapamycin for additional 12 h. The cells were solubilized with the extraction buffer, and the cell lysate was immunoprecipitated with anti-HA affinity

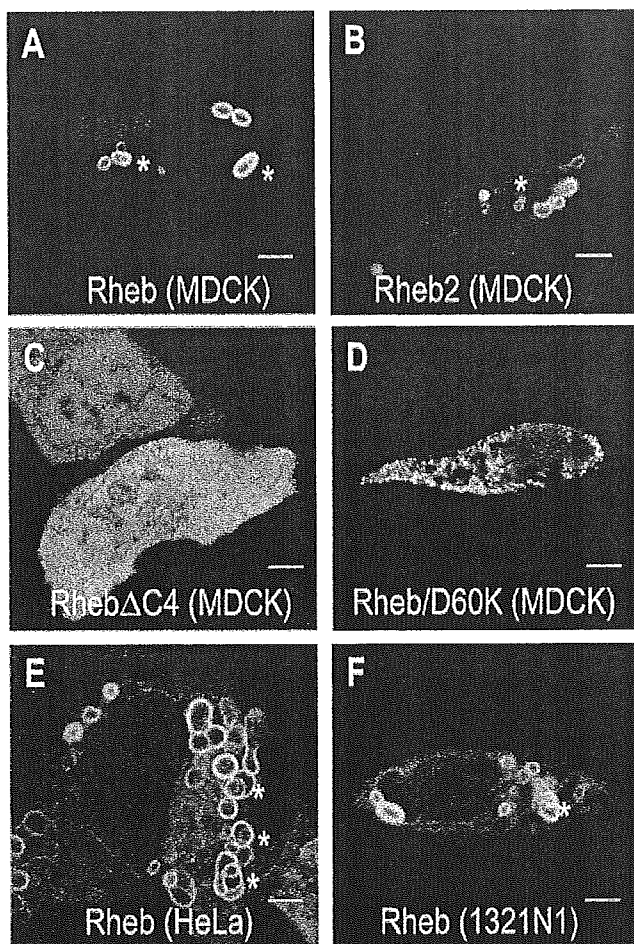


Fig. 2. Rheb and Rheb2 induce large vacuole formation. MDCK cells were transfected with EGFP-Rheb (A), EGFP-Rheb2 (B), EGFP-Rheb Δ C4 (C), or EGFP-Rheb/D60K (D) and cultured for 16 h. HeLa (E) and 1321N1 astrocytoma (F) cells were also transfected with EGFP-Rheb. These cells were analyzed by a confocal microscopy as described under Experimental Procedures. Scale bars indicate 5 μ m, and asterisks show the multi-lamellar and multi-vesicular structures.

matrix (Roche). The immunocomplexes were washed five times with a buffer consisting of 20 mM Tris-HCl (pH 7.5), 2 mM EDTA, 100 mM NaCl, and 0.4% Triton X-100, and the precipitated proteins were subjected to SDS-PAGE and Western blotting with anti-p70 (Santa Cruz Biotechnology) and anti-phosphorylated p70 (Cell Signaling) S6K antibodies.

All experiments were repeated at least three times with different batches of the cell samples, and the results were fully reproducible. Hence, most of the data shown are representative of several independent experiments.

RESULTS AND DISCUSSION

Rheb and Rheb2 mRNAs Are Differently Distributed in Human Tissues—In addition to Rheb (Rheb1), human Rheb2 cDNA was recently identified (4). To investigate the distribution patterns of Rheb and Rheb2 mRNAs in various human tissues, Northern blot analysis was per-

formed with a radiolabeled probe containing full-length sequences of Rheb and Rheb2. As shown in Fig. 1A, a 1.6-kb Rheb transcript was observed in various human tissues in accordance with a previous report (3). In contrast, a 1.6-kb Rheb2 transcript was observed predominantly in the brain and less in the spleen and peripheral blood. Because of the highly sequence homology between Rheb and Rheb2 mRNAs, the specificity of each probe was confirmed by the following analysis. Nitrocellulose membranes were blotted with Rheb and Rheb2 plasmids and hybridized with both probes. Specific signals were observed only when their RNAs were hybridized with the corresponding probes (data not shown). Thus, no cross-hybridization between Rheb and Rheb2 was detected under the present conditions. We next examined the distributions of Rheb and Rheb2 mRNAs in specific brain regions. Rheb was found to be expressed in all brain regions, while Rheb2 mRNA was restricted to the cerebral cortex, occipital pole, frontal and temporal lobes (Fig. 1B). Rheb2 is present only in mammalian cells, although Rheb is highly conserved among various species. Thus, Rheb2 may have a specific role in the brain region of higher eukaryotes, of which activation might lead to epilepsy, which is a typical pathology of TSC patients.

Rheb Induces Large Vacuole Formation—To determine the intracellular localization of Rheb and Rheb2 in living cells, EGFP-tagged proteins were expressed in MDCK cells, and their distributions were analyzed by confocal microscopy (Fig. 2, A–D). Interestingly, the expression of Rheb and Rheb2 induced the formation of large vacuoles dispersed throughout the cells, and the proteins localized to the vacuole membranes (see panels A and B). In contrast, the expression of a mutant Rheb, Rheb Δ C4, which lacks the carboxy-terminal membrane-anchoring sequence CAAX, give rise to diffused signals and did not induce such large vacuoles (Fig. 2C). Enlarged vacuoles were also induced upon the expression of EGFP-tagged Rheb in HeLa, 1321N1 human astrocytoma cells (Fig. 2, E and F) and 293 cells (see Figs. 5B and 6B, control cells). As shown by the asterisks in Fig. 2, these vacuoles often had multi-lamellar structures, which are characteristic of late endocytic vesicles (late endosome and lysosome).

Rheb Localizes to Endocytic Rab7- and Rab9-Positive Vesicles—To identify the nature of the large vacuoles in which Rheb localized, some members of the Rab GTPase family tagged with Dsred were simultaneously expressed in MDCK cells as organelle markers specific for each subcellular compartment. As shown in Fig. 3, A and D, Rab5 and Rab11, which are involved in early endosome formation and endosomal recycling, respectively, showed distinct staining patterns from Rheb. On the other hand, Rab7 and Rab9, used as late endocytic markers, mostly co-localized with Rheb in the enlarged vacuoles (Fig. 3, B and C). These data correlate with the observation that Rheb localizes in the multi-lamellar late endocytic vesicles. When the amount of Rheb transfected was increased, we observed partial co-localization of Rab5 in the Rheb-induced vacuoles (data not shown), suggesting that hybrids of early and late endocytic organelles were created.

Vacuole Formation Is Affected by the GTPase Cycle of Rheb—Rheb has been characterized as a unique small GTPase in which critical amino acids necessary for

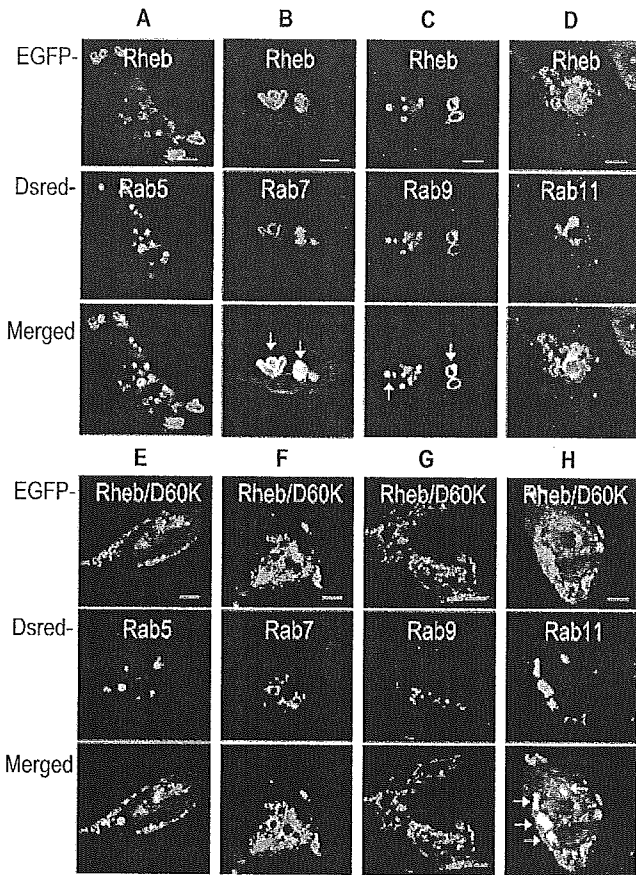
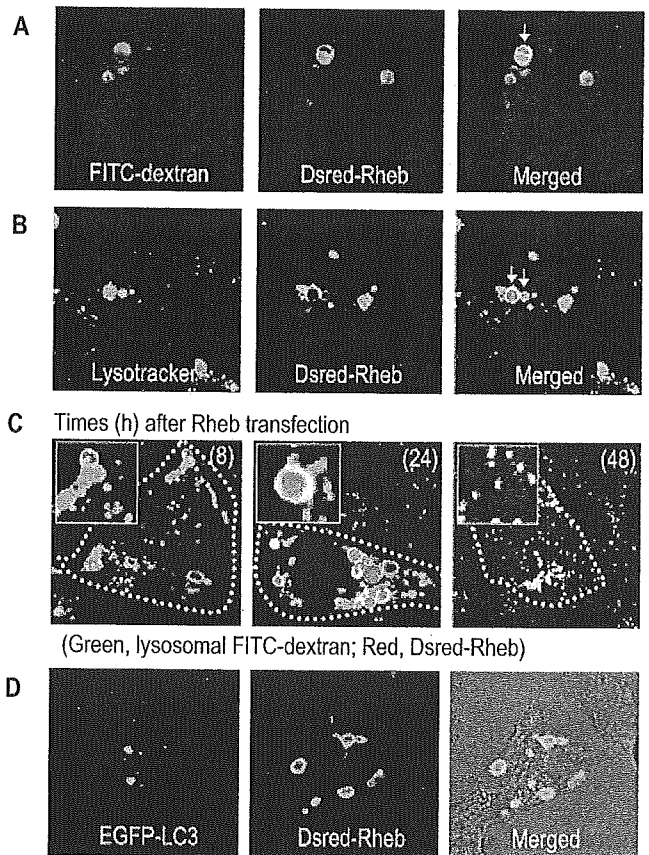


Fig. 3. Rheb co-localizes with Rab7 and Rab9 in multi-vesicular structures, whereas Rheb/D60K mutant co-localizes partly with Rab11-containing vesicles. MDCK cells were transfected with EGFP-Rheb (A–D) or EGFP-Rheb/D60K (E–H), together with Dsred-Rab5 (A and E), Dsred-Rab7 (B and F), Dsred-Rab9 (C and G) or Dsred-Rab11 (D and H), and further incubated for 16 h. The fluorescence of EGFP (upper) and Dsred (middle) was visualized by the confocal microscopy. Merged images of the two signals are also illustrated (bottom). Scale bars indicate 5 μ m.

Fig. 4. Rheb-positive vesicles are translocated from late endosomes to lysosomes. A and B, MDCK cells transfected with Dsred-Rheb (A and B) were incubated with 1 mg/ml of FITC-dextran for 12 h (A) or 50 nM LysoTracker Green for 1 h (B). C, MDCK cells, of which lysosomal fractions had been labeled with FITC-dextran, were transfected with Dsred-Rheb and further incubated for the indicated times. The left upper insets show the enlargement of a part of the images, and the white dotted line indicates a single Rheb-transfected cell. D, MDCK cells were transfected with EGFP-LC3 and Dsred-Rheb and cultured for 16 h. The fluorescent and merged images are illustrated.



GTPase reaction are not conserved (3). This implies that Rheb may exist in living cells mostly as a GTP-bound form (1). Furthermore, a mutant Rheb, Rheb/D60K, has recently been reported to exhibit a dominant-negative effect on the activation of the mTOR pathway (24). To confirm the nucleotide-bound status of the wild-type and mutant Rhebs, HeLa cells were transfected with the FLAG-tagged proteins and cultured in $^{32}\text{P}_i$ -containing medium. The recombinant proteins were immunoprecipitated, and the radiolabeled nucleotides associating with the proteins were analyzed by thin-layer chromatography. As expected, wild-type Rheb and Rheb/D60K existed mostly as GTP-bound and GDP-bound forms, respectively (data not shown).

We next examined how the nucleotide-bound forms of Rheb are localized in MDCK cells. In contrast to wild-type Rheb (see Fig. 2A), the expression of Rheb/D60K did not induce large vacuoles, but the mutant protein localized in intracellular small vesicles (Fig. 2D). As shown in Fig. 3, F and G, co-staining with Rab7 and Rab9 revealed that Rheb/D60K localized was quite differently from the wild-type protein, but abutting on late endocytic vesicles (compare with B and C). Rab5 also did not co-localize with the Rheb/D60K signals (E). However, recycling endosomes associating with Rab11 showed partial co-localization with Rheb/D60K (H). It should be noted here that the vesicular localization of each Rab protein was not markedly affected by the transfection of the wild-type or the mutant Rheb proteins (compare panels A–D with E–H). These data suggest that the subcellular localization of Rheb changed depending on its nucleotide-bound state.

Rheb-Positive Vesicles Are Translocated from Late Endosomes to Lysosomes—We further investigated how the Rheb-positive vesicles are created in the membrane trafficking pathway by comparing the localization of various endocytic makers. As shown in Fig. 4A, FITC-dextran, which is a non-selective endocytic marker that is able to reach late endosomes and lysosomes, was found to be present partly in lumens of the Rheb-positive vesicles. LysoTracker, a labeling probe for acidic organelles such as lysosomes (25), also accumulated in the Rheb-positive structures (Fig. 4B), indicating that parts of the Rheb-positive vesicles had acidic characteristics. We also investigated the time-dependent formation of Rheb-positive vesicles in MDCK cells, of which the lysosomal fraction had been selectively labeled with FITC-dextran. As shown in Fig. 4C, Rheb-positive vesicles were evident at 8 h after the transfection, but their distribution never co-localized with FITC-dextran, indicating that the early stage of expressed Rheb is not present in lysosomes. However, some Rheb signals co-localized with the FITC-dextran at 24 h, and most of the Rheb signals moved to the FITC-labeled lysosome at 48 h, suggesting that Rheb vesicles are gradually translocated to lysosomal compartments. These results are consistent with the previous results showing the co-localization of Rheb with Rab7 and Rab9 (see Fig. 3, B and C). Thus, the Rheb-positive vesicles appeared to be created at least from endocytic (or unidentified) organelles and gradually to fuse with lysosomes through late endosomes.

To further confirm the late endocytic localization of Rheb signals, we attempted to immunostain the Rheb-

transfected cells with antibodies specific for late endocytic organelles. However, the Rheb-containing vesicles were fragmented during the process of fixation, and the localization of Rheb in the fixed cells appeared to be different from that in the living cells (data not shown). We could not overcome this problem with any of several fixation methods tested. Nevertheless, we would like to propose that the Rheb-induced vesicles have characteristics of late endocytic organelles based on the following observations. First, Rheb could co-localize with Rab7 and Rab9 but not with Rab5 or Rab11. Second, Rheb-induced organelles contained the endocytic marker FITC-dextran. Third, Rheb-induced vesicles were characterized as acidic organelles. Fourth, Rheb-containing vesicles gradually became positive for lysosomal markers.

The Rheb-positive vesicles seemed to share similar characteristics with autophagosomes in terms of Rab7-positive, lysosome-fusible, and multi-lamellar structures (26, 27). Moreover, mTOR, which is a downstream kinase of Rheb GTPase, appears to function as a negative regulator of autophagy (17, 28). Therefore, we analyzed whether Rheb signals co-localize with the autophagosome marker LC3, since Rheb-positive structures might be parts of accumulated incomplete autophagosomes due to the inhibition of autophagy through the activation of mTOR kinase. However, EGFP-LC3 signals never co-localized with Dsred-Rheb (Fig. 4D). When the transfected cells were starved by serum depletion, there was a marked elevation of the LC3 signals lacking co-localization with Rheb (data not shown). These data suggest that Rheb-positive vesicles are different entities from autophagosomes.

PI3k-Akt Signaling May Be Involved in the Upstream Pathway of the Rheb-Induced Vacuole Formation—As mentioned before, PI3k-Akt signaling appears to be involved in the upstream pathway of Rheb activation. To investigate whether inhibition of PI3k affects the Rheb-induced vacuole formation, the transfected 293 cells were incubated with the specific inhibitor LY294002, under which conditions PI3k activity was entirely suppressed. The effectiveness of the sustained PI3k inhibition was confirmed by measuring the phosphorylation of GSK-3 β , a direct substrate of Akt. As shown in Fig. 5A, the inhibition of PI3k was clearly evident even after incubation of the cells with LY294002 for 16 h. Under these conditions, Rheb-induced large vacuole formation was markedly impaired in 293 cells (Fig. 5B). Instead, small punctated Rheb-positive vesicles were evident in the LY294002-treated cells, which are reminiscent of Rheb/D60K-induced vesicles (see Fig. 2D). This suggests that LY294002 probably activates endogenous GAP, so that expressed Rheb is rapidly deactivated and fails to induce large vacuoles under these conditions. These results may indicate that PI3k-Akt signaling is situated in the upstream of the pathway involved in the large vacuole formation. However, the PI3k activity has been also known to regulate various aspects of endosomal and lysosomal functions and membrane trafficking independent of Rheb functions (29). Thus, the GAP-sensitive GTPase cycle of Rheb appears to partly regulate the endocytic pathway from late endosomes to lysosomes, although we can not totally rule out the possibility that impaired vacuole formation in LY294002-treated cells is due to the inhibition of other

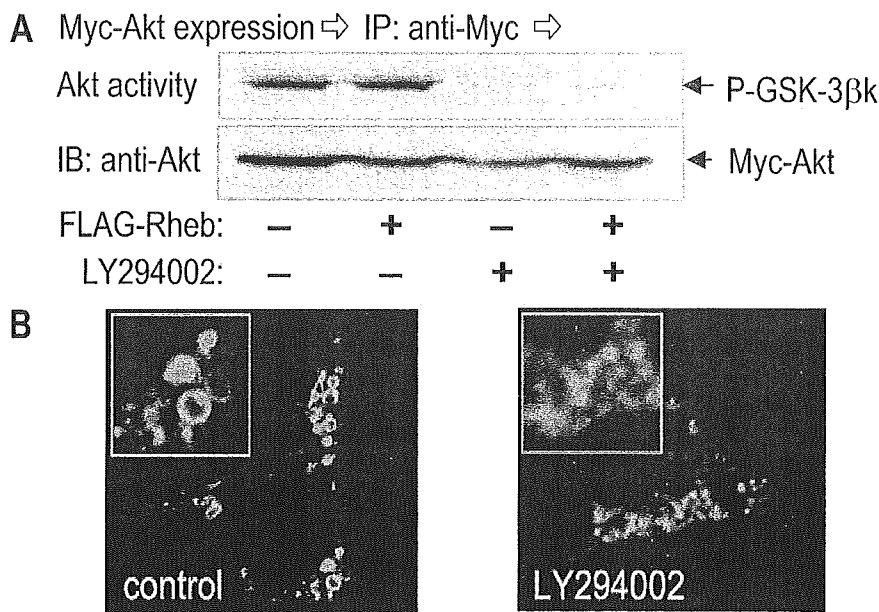


Fig. 5. PI3k-Akt signaling may be involved in the Rheb-induced vacuole formation. 293 cells that had been transfected with Myc-Akt and FLAG-Rheb (A) or Dsred-Rheb (B) were incubated in the presence or absence of 50 μ M LY294002. A, the cell lysates were prepared and subjected to immunoprecipitation (IP) with an anti-Myc antibody, and the kinase activity and protein amount of Akt in the precipitated fractions were measured as described under "MATERIALS AND METHODS." B, the fluorescence of Dsred was visualized by confocal microscopy. The left upper insets show the enlargement of a part of the images.

endosomal target(s), which is regulated by the activity of PI3k.

Rheb-Induced Vacuolar Formation Is Independent of the Activation of mTOR—It has been reported that Rheb stimulates the kinase activity of mTOR, which leads to the activation of S6K responsible for protein synthesis (16). To investigate whether the activation of mTOR kinase is necessary for the induction of Rheb-positive vacuoles, 293 cells were transfected with FLAG-Rheb under conditions whereby mTOR activity was entirely suppressed with the specific inhibitor rapamycin. The effectiveness of the mTOR inhibition was confirmed by

measuring the phosphorylation of p70 S6K, a direct substrate of mTOR. As shown in Fig. 6A, the inhibition of mTOR was clearly observed even after prolonged incubation of the cells with rapamycin. However, there was no marked difference in the Rheb-positive vacuole formation between the control and rapamycin-treated cells (Fig. 6B). These data indicate that the activation of mTOR is not required for the Rheb-induced vacuole formation.

The Possible Role of Rheb-Induced Vacuole Formation in Cell Functions Other than Cell Growth and Cell-Cycle Progression—The present study has revealed that Rheb activation induces large vacuoles in cytoplasm of the

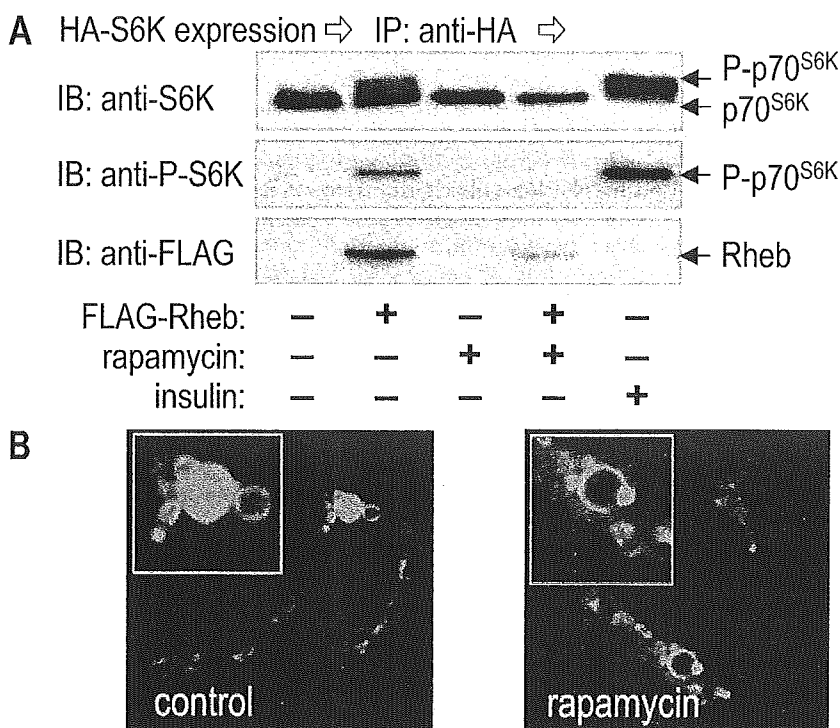


Fig. 6. Activation of mTOR kinase is not required for the Rheb-induced vacuole formation. 293 cells that had been transfected with FLAG-Rheb and HA-p70 S6K (A) or Dsred-Rheb (B) were incubated in the presence or absence of 40 nM rapamycin. A, as a control, the transfected HA-p70 S6 kinase was stimulated by incubation of cells with 200 nM insulin. Cell lysates were prepared and immunoprecipitated with an anti-HA antibody. The precipitated fractions were separated by SDS-PAGE and subjected to immunoblot analysis with anti-p70 S6K (upper) or anti-phosphorylated p70 S6K (middle) antibodies. The cell lysates were also immunoblotted with an anti-FLAG antibody (bottom). B, the fluorescence of Dsred was visualized by confocal microscopy. The left upper insets show the enlargement of a part of the images.

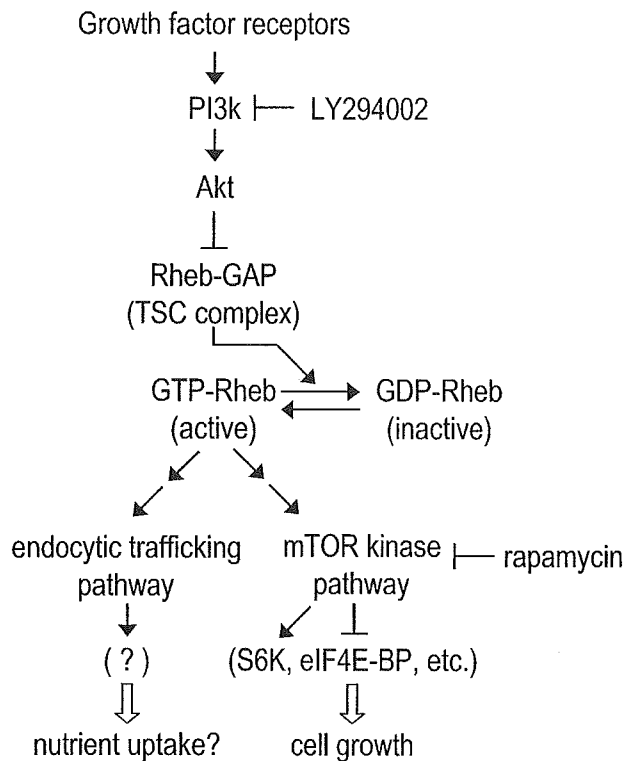


Fig. 7. Schematic representation of Rheb-related signal transduction pathways. Rheb induces not only the activation of mTOR kinase leading to cell growth but also late-endocytic vesicle formation that may play a critical role in nutrient uptake. See text for further explanation.

transfected cells and that the vacuoles are characterized as late endosome- or lysosome-like organelles. Moreover, the large vacuole formation is dependent on the GTPase cycle of Rheb and probably the stimulation of the PI3k-Akt pathway, but not on the activation of mTOR kinase. These data suggest that Rheb-induced vacuole formation is a novel Rheb-downstream pathway that is distinguishable from the activation of mTOR kinase pathway (Fig. 7). Rheb was first identified as a gene whose mRNA expression is increased in rat brain by seizures or by the stimulation of long-term potentiation (3). Since then, several groups has examined whether Rheb is involved in the activation of Raf, the well-known downstream kinase of conventional Ras (30–33). The recent identification of Rheb as a positive regulator of mTOR pathway has attracted considerable attention, in addition to the report that TSC acts as a GAP for Rheb (1, 15, 34, 35). To our knowledge, however, this is the first report that indicates the involvement of Rheb in the endocytic pathway.

In yeast, several reports suggest that TSC positively and Rheb negatively regulate arginine uptake (18–20). In addition, Tsc1 and Tsc2 knockouts in *S. pombe* exhibited abnormal intracellular distribution of an amino-acid permease (21). It is, therefore, tempting to speculate that the activation of Rheb induces endocytic vacuoles that may have an effect on the localization of permeases. Our preliminary experiments indicate that Rheb is capable of interacting directly with several channels or transporters

implicated in nutrient uptake. Moreover, these transporters were selectively translocated from the plasma membrane to Rheb-induced vacuoles in Rheb-transfected cells. These results suggest that Rheb-induced vacuoles are necessary for nutrient regulation through their translocation (Fig. 7). Further investigation is needed to uncover the physiological roles of Rheb, and it is important to investigate the regulation of the endocytic pathway in terms of nutrient uptake, in which Rheb-pathway may play a critical role.

This work was supported in part by research grants from the Ministry of Education, Culture, Sports, Science and Technology (MEXT) of the Japanese Government, the Japan Society for the Promotion of Science (JSPS), the Mitsubishi Foundation, and the Uehara Memorial Foundation.

REFERENCES

- Li, Y., Corradetti, M.N., Inoki, K., and Guan, K.L. (2004) TSC2: filling the GAP in the mTOR signaling pathway. *Trends Biochem. Sci.* **29**, 32–38
- Kontani, K., Tada, M., Ogawa, T., Okai, T., Saito, K., Araki, Y., and Katada, T. (2002) Di-Ras, a distinct subgroup of ras family GTPases with unique biochemical properties. *J. Biol. Chem.* **277**, 41070–41078
- Yamagata, K., Sanders, L.K., Kaufmann, W.E., Yee, W., Barnes, C.A., Nathans, D., and Worley, P.F. (1994) rheb, a growth factor- and synaptic activity-regulated gene, encodes a novel Ras-related protein. *J. Biol. Chem.* **269**, 16333–16339
- Patel, P.H., Thapar, N., Guo, L., Martinez, M., Maris, J., Gau, C.L., Lengyel, J.A., and Tamanoi, F. (2003) *Drosophila* Rheb GTPase is required for cell cycle progression and cell growth. *J. Cell Sci.* **116**, 3601–3610
- Inoki, K., Li, Y., Xu, T., and Guan, K.L. (2003) Rheb GTPase is a direct target of TSC2 GAP activity and regulates mTOR signaling. *Gene Dev.* **17**, 1829–1834
- Garami, A., Zwartkruis, F.J., Nobukuni, T., Joaquin, M., Rocco, M., Stocker, H., Kozma, S.C., Hafen, E., Bos, J.L., and Thomas, G. (2003) Insulin activation of Rheb, a mediator of mTOR/S6K/4E-BP signaling, is inhibited by TSC1 and 2. *Mol. Cell* **11**, 1457–1466
- Castro, A.F., Rebhun, J.F., Clark, G.J., and Quilliam, L.A. (2003) Rheb binds tuberous sclerosis complex 2 (TSC2) and promotes S6 kinase activation in a rapamycin- and farnesylation-dependent manner. *J. Biol. Chem.* **278**, 32493–32496
- Tee, A.R., Manning, B.D., Roux, P.P., Cantley, L.C., and Blenis, J. (2003) Tuberous sclerosis complex gene products, Tuberin and Hamartin, control mTOR signaling by acting as a GTPase-activating protein complex toward Rheb. *Curr. Biol.* **13**, 1259–1268
- Saucedo, L.J., Gao, X., Chiarelli, D.A., Li, L., Pan, D., and Edgar, B.A. (2003) Rheb promotes cell growth as a component of the insulin/TOR signalling network. *Nat. Cell Biol.* **5**, 566–571
- Stocker, H., Radimerski, T., Schindelholz, B., Wittwer, F., Belawat, P., Daram, P., Breuer, S., Thomas, G., and Hafen, E. (2003) Rheb is an essential regulator of S6K in controlling cell growth in *Drosophila*. *Nat. Cell Biol.* **5**, 559–565
- Zhang, Y., Gao, X., Saucedo, L.J., Ru, B., Edgar, B.A., and Pan, D. (2003) Rheb is a direct target of the tuberous sclerosis tumour suppressor proteins. *Nat. Cell Biol.* **5**, 578–581
- Franke, T.F., Yang, S.I., Chan, T.O., Datta, K., Kazlauskas, A., Morrison, D.K., Kaplan, D.R., and Tsichlis, P.N. (1995) The protein kinase encoded by the Akt proto-oncogene is a target of the PDGF-activated phosphatidylinositol 3-kinase. *Cell* **81**, 727–736
- Burgering, B.M. and Coffey, P.J. (1995) Protein kinase B (c-Akt) in phosphatidylinositol-3-OH kinase signal transduction. *Nature* **376**, 599–602

14. Inoki, K., Li, Y., Zhu, T., Wu, J., and Guan, K.L. (2002) TSC2 is phosphorylated and inhibited by Akt and suppresses mTOR signalling. *Nat. Cell Biol.* **4**, 648–657
15. Manning, B.D. and Cantley, L.C. (2003) Rheb fills a GAP between TSC and TOR. *Trends Biochem. Sci.* **28**, 573–576
16. Fingar, D.C. and Blenis, J. (2004) Target of rapamycin (TOR): an integrator of nutrient and growth factor signals and coordinator of cell growth and cell cycle progression. *Oncogene* **23**, 3151–3171
17. Raught, B., Gingras, A.C., and Sonenberg, N. (2001) The target of rapamycin (TOR) proteins. *Proc. Natl Acad. Sci. USA* **98**, 7037–7044
18. van Slegtenhorst, M., Carr, E., Stoyanova, R., Kruger, W.D., and Henske, E.P. (2004) Tsc1+ and tsc2+ regulate arginine uptake and metabolism in *Schizosaccharomyces pombe*. *J. Biol. Chem.* **279**, 12706–12713
19. Urano, J., Tabancay, A.P., Yang, W., and Tamanoi, F. (2000) The *Saccharomyces cerevisiae* Rheb G-protein is involved in regulating canavanine resistance and arginine uptake. *J. Biol. Chem.* **275**, 11198–11206
20. Mach, K.E., Furge, K.A., and Albright, C.F. (2000) Loss of Rhb1, a Rheb-related GTPase in fission yeast, causes growth arrest with a terminal phenotype similar to that caused by nitrogen starvation. *Genetics* **155**, 611–622
21. Matsumoto, S., Bandyopadhyay, A., Kwiatkowski, D.J., Maitra, U., and Matsumoto, T. (2002) Role of the Tsc1-Tsc2 complex in signaling and transport across the cell membrane in the fission yeast *Schizosaccharomyces pombe*. *Genetics* **161**, 1053–1063
22. Saito, K., Murai, J., Kajiho, H., Kontani, K., Kurosu, H., and Katada, T. (2002) A novel binding protein composed of homophilic tetramer exhibits unique properties for the small GTPase Rab5. *J. Biol. Chem.* **277**, 3412–3418
23. Kajiho, H., Saito, K., Tsujita, K., Kontani, K., Araki, Y., Kurosu, H., and Katada, T. (2003) RIN3: a novel Rab5 GEF interacting with amphiphysin II involved in the early endocytic pathway. *J. Cell Sci.* **116**, 4159–4168
24. Tabancay, A.P., Jr., Gau, C.L., Machado, I.M., Uhlmann, E.J., Gutmann, D.H., Guo, L., and Tamanoi, F. (2003) Identification of dominant negative mutants of Rheb GTPase and their use to implicate the involvement of human Rheb in the activation of p70S6K. *J. Biol. Chem.* **278**, 39921–39930
25. Bucci, C., Thomsen, P., Nicoziani, P., McCarthy, J., and van Deurs, B. (2000) Rab7: a key to lysosome biogenesis. *Mol. Biol. Cell* **11**, 467–480
26. Gutierrez, M., Munafo, D., Beron, W., and Colombo, M. (2004) Rab7 is required for the normal progression of the autophagic pathway in mammalian cells. *J. Cell Sci.* **117**, 2687–2697
27. Gozuacik, D. and Kimchi, A. (2004) Autophagy as a cell death and tumor suppressor mechanism. *Oncogene* **23**, 2891–2906
28. Kamada, Y., Sekito, T., and Ohsumi, Y. (2004) Autophagy in yeast: a TOR-mediated response to nutrient starvation. *Curr. Top. Microbiol. Immunol.* **279**, 73–84
29. Simonsen, A., Wurmser, A.E., Emr, S.D., and Stenmark, H. (2001) The role of phosphoinositides in membrane transport. *Curr. Opin. Cell Biol.* **13**, 485–492
30. Clark, G.J., Kinch, M.S., Rogers-Graham, K., Sebt, S.M., Hamilton, A.D., and Der, C.J. (1997) The Ras-related protein Rheb is farnesylated and antagonizes Ras signaling and transformation. *J. Biol. Chem.* **272**, 10608–10615
31. Yee, W.M. and Worley, P.F. (1997) Rheb interacts with Raf-1 kinase and may function to integrate growth factor- and protein kinase A-dependent signals. *Mol. Cell Biol.* **17**, 921–933
32. Im, E., von Lintig, F.C., Chen, J., Zhuang, S., Qui, W., Chowdhury, S., Worley, P.F., Boss, G.R., and Pilz, R.B. (2002) Rheb is in a high activation state and inhibits B-Raf kinase in mammalian cells. *Oncogene* **21**, 6356–6365
33. Karbowniczek, M., Cash, T., Cheung, M., Robertson, G.P., Astrinidis, A., and Henske, E.P. (2004) Regulation of B-Raf kinase activity by tuberin and Rheb is mammalian target of rapamycin (mTOR)-independent. *J. Biol. Chem.* **279**, 29930–29937
34. Pan, D., Dong, J., Zhang, Y., and Gao, X. (2004) Tuberous sclerosis complex: from *Drosophila* to human disease. *Trends Cell Biol.* **14**, 78–85
35. Aspuria, P. and Tamanoi, F. (2004) The Rheb family of GTP-binding proteins. *Cell Signal.* **16**, 1105–1112

Tsuyoshi Ishikawa · Shuji Terai · Yohei Urata ·
Yoshio Marumoto · Koji Aoyama · Isao Sakaida ·
Tomoaki Murata · Hiroshi Nishina · Koh Shinoda ·
Shunji Uchimura · Yoshihiko Hamamoto ·
Kiwamu Okita

Fibroblast growth factor 2 facilitates the differentiation of transplanted bone marrow cells into hepatocytes

Received: 25 May 2005 / Accepted: 9 August 2005
© Springer-Verlag 2005

Abstract We have developed an in vivo mouse model, the green fluorescent protein (GFP)/carbon tetrachloride (CCl₄) model, and have previously reported that transplanted GFP-positive bone marrow cells (BMCs) differentiate into hepatocytes via hepatoblast intermediates. Here, we have investigated the growth factors that are

closely related to the differentiation of transplanted BMCs into hepatocytes, and the way that a specific growth factor affects the differentiation process in the GFP/CCl₄ model. We performed immunohistochemical analysis to identify an important growth factor in our model, viz., fibroblast growth factor (FGF). In liver samples, the expression of FGF1 and FGF2 and of FGF receptors (FGFRs; FGFR1, FGFR2) was significantly elevated with time after bone marrow transplantation (BMT) compared with other factors, and co-expression of GFP and FGFs or FGFRs could be detected. We then analyzed the effect and molecular mechanism of FGF signaling on the enhancement of BMC differentiation into hepatocytes by immunohistochemistry, immunoblotting, and microarray analysis. Treatment with recombinant FGF (rFGF), especially rFGF2, elevated the repopulation rate of GFP-positive cells in the liver and significantly increased the expression of both Liv2 (hepatoblast marker) and albumin (hepatocyte marker). Administration of rFGF2 at BMT also raised serum albumin levels and improved the survival rate. Transplantation of BMCs with rFGF2 specifically activated tumor necrosis factor- α (TNF- α) signaling. Thus, FGF2 facilitates the differentiation of transplanted BMCs into albumin-producing hepatocytes via Liv2-positive hepatoblast intermediates through the activation of TNF- α signaling. Administration of FGF2 in combination with BMT improves the liver function and prognosis of mice with CCl₄-induced liver damage.

This study was supported by Grants-in-Aid for Scientific Research from the Japan Society for the Promotion of Science (nos. 13470121, 13770262, 15790348, 16390211, and 16590597) and for translational research from the Ministry of Health, Labor and Welfare (H-trans-5).

T. Ishikawa · S. Terai (✉) · Y. Urata · Y. Marumoto ·
K. Aoyama · I. Sakaida · K. Okita
Department of Molecular Science & Applied Medicine
(Gastroenterology & Hepatology),
Yamaguchi University School of Medicine,
Minami Kogushi 1-1-1, Ube,
755-8505 Yamaguchi, Japan
e-mail: terais@yamaguchi-u.ac.jp
Tel.: +81-836-222241
Fax: +81-836-222240

T. Murata
Science Research Center, Yamaguchi University,
Minami Kogushi 1-1-1, Ube,
755-8505 Yamaguchi, Japan

H. Nishina
Department of Developmental and Regenerative Biology,
Medical Research Institute,
Tokyo Medical and Dental University,
1-5-45, Yushima, Bunkyo-ku,
Tokyo, 113-8510, Japan

K. Shinoda
Department of Neuroanatomy & Neuroscience,
Yamaguchi University School of Medicine,
Minami Kogushi 1-1-1, Ube,
755-8505 Yamaguchi, Japan

S. Uchimura · Y. Hamamoto
Department of Computer Science and Systems Engineering,
Faculty of Engineering, Yamaguchi University,
Tokiwadai 2-16-1, Ube,
755-8611 Yamaguchi, Japan

Keywords Bone marrow cell · Stem cell · Hepatocyte ·
Differentiation · Liver · Fibroblast growth factor ·
Tumor necrosis factor · Mouse

Abbreviations BMC: bone marrow cell · BMT: bone marrow transplantation · GFP: green fluorescent protein · CCl₄: carbon tetrachloride · SOM: self-organizing map · FGF: fibroblast growth factor · EGF: epidermal growth factor · EGFR: epidermal growth factor receptor · FGFR: fibroblast growth factor receptor · HGF: hepatocyte growth factor · VEGF: vascular endothelial growth factor · VEGFR: vascular endothelial growth factor receptor ·

PDGF: platelet-derived growth factor · PDGFR: platelet-derived growth factor receptor · TGF β : transforming growth factor β · TGF β R: transforming growth factor β receptor · rFGF: recombinant fibroblast growth factor · TNF- α : tumor necrosis factor- α · TNFIP3: tumor necrosis factor- α induced protein 3 · NF- κ B: nuclear factor- κ B

Introduction

Liver cirrhosis is the end-stage of chronic liver disease and is extremely difficult to treat. Currently, liver transplantation is one of the effective therapies available to patients who face this life-threatening condition. However, this treatment presents serious problems, such as the lack of a donor, operative damage, rejection, and high cost. Regenerative therapy by stem cell transplantation is a promising approach for the treatment of patients with severe liver disease. The capacity of bone marrow cells (BMCs) to differentiate into hepatocytes and intestinal cells was first identified through the detection of Y-chromosome-containing cells in postmortem samples from female recipients of BMCs from male donors (Alison et al. 2000; Theise et al. 2000). Bone marrow transplantation (BMT) is now an established treatment for hematological diseases, and several clinical studies have evaluated the potential of BMCs in regeneration of the myocardium and blood vessels (Orlic et al. 2001; Stamm et al. 2003; Wexler et al. 2003). Together, these findings suggest that BMCs will be an effective cell source for regenerative therapy in the liver.

To realize the potential for cell therapy by BMCs, we have developed an *in vivo* mouse model to monitor the differentiation of BMCs into hepatocytes, *viz.*, the green fluorescent protein (GFP)/carbon tetrachloride (CCl₄) model (Terai et al. 2003). We have shown that transplanted GFP-positive BMCs populate the damaged liver and differentiate into albumin-producing hepatocytes via hepatoblast intermediates under CCl₄-induced persistent liver-damage conditions (Terai et al. 2003; Yamamoto et al. 2004). Furthermore, BMT elevates serum albumin levels, reduces liver fibrosis, and improves the survival rate of CCl₄-treated mice (Sakaida et al. 2004). These results suggest that BMT could become an effective treatment for patients with liver failure.

Several lines of evidence support the idea that chronic liver injury by CCl₄ is required to induce the differentiation of transplanted stem cells into hepatocyte-like cells (Wang et al. 2003; Kollet et al. 2003). In our model, similarly, some feature associated with continuous intraperitoneal administration of CCl₄, which causes persistent liver damage, actually appears to facilitate or induce migration of BMCs to the liver and differentiation of BMCs into hepatocytes. In addition, we have used microarray analysis, together with a self-organizing map (SOM), to show that dramatic gene activation occurs after BMT into mice with CCl₄-induced liver damage (Omori et al. 2004). Genes associated with morphology are activated at an early stage, whereas genes that regulate differentiation of hepatocytes are up-regulated at a later stage.

Growth factors are known to affect cell proliferation and differentiation and reportedly participate in repair processes of many organs. Moreover, clinical trials have been carried out with several growth factors for the therapy of peripheral vascular disorders, ischemic heart diseases, and cutaneous chronic wounds through neoangiogenesis (Laham et al. 2000; Lederman et al. 2002; Fu et al. 2002). Here, we report the identification of a growth factor that induces cellular repopulation of damaged liver and the differentiation of transplanted BMCs into hepatocytes. Furthermore, we report the results of our investigation into the way that the identified growth factor, namely fibroblast growth factor (FGF), affects these processes in the GFP/CCl₄ mouse model of liver damage and regenerative treatment.

Materials and methods

Experimental protocol: GFP/CCl₄ model

C57 BL/6 Tg14 (act-EGFP) OsbY01 mice (GFP transgenic mice) were kindly provided by Dr. Masaru Okabe (Genome Research Center, Osaka University, Osaka, Japan), and C57 BL/6 female mice were purchased from Japan SLC (Shizuoka, Japan). In this study, injection of 1.0 ml/kg body weight of CCl₄ into recipient mice was performed at 6 weeks of age via the peritoneum twice a week for 4 weeks to induce persistent liver damage. On one day after 4 weeks of CCl₄ treatment, 1 \times 10⁵ GFP-positive BMCs were transplanted slowly, by using a 31-gauge needle and Hamilton syringe, via the tail vein as previously described (Terai et al. 2003). After BMT, the same dose of CCl₄ was continuously injected twice a week to maintain persistent liver damage. Mice treated with CCl₄ without BMT were used as a control group. Individual mice were killed at 48 h and every week after BMT. All processes, including surgical steps, conformed to the guidelines of Yamaguchi University for animal and recombinant DNA experiments.

Immunohistochemical staining

We obtained liver samples from six independent mice in each group, and immunohistochemical staining was performed as previously described (Shinoda et al. 1992). Immunohistochemical samples were quantified by using a Provis microscope (Olympus, Tokyo, Japan) equipped with a charge-coupled device camera; the obtained images were subjected to computer-assisted analysis with MetaMorph software (Universal Imaging, Downingtown, Pa.). A total of 30 random fields per group were analyzed independently, and the percentage of stained area was calculated by using MetaMorph software. For screening, we examined the expression of several growth factor receptors by using commercial antibodies against the following: epidermal growth factor (EGF) receptor (EGFR), FGF receptor 1 (FGFR1), and FGFR2, all from Santa Cruz Biotechnology (Calif., USA); hepatocyte growth factor (HGF) receptor (c-Met) from R&D Systems (Minn., USA); vascular

endothelial growth factor (VEGF) receptor 1 (VEGFR1), VEGFR2, platelet-derived growth factor (PDGF) receptor α (PDGFR α), PDGFR β , transforming growth factor β (TGF β) receptor 1 (TGF β R1), and TGF β R2, all from Santa Cruz Biotechnology. In addition, we analyzed the expression of FGFRs and FGFs by using antibodies against FGFR1, FGFR2, FGF1, and FGF2 (Santa Cruz Biotechnology) in two groups: the BMT(+) group that received both CCl₄ treatment and BMT, and the BMT(-) control group that received CCl₄-only treatment without BMT. Immunofluorescent detection of GFP and FGFRs or FGFs was performed with the following secondary antibodies: Alexa Fluor R-488 and R-568 donkey anti-goat IgG (H+L) conjugates and Alexa Fluor R-488 goat anti-rabbit IgG (H+L) conjugate (Molecular Probes, Eugene, Ore., USA). The analysis was performed as previously described (Terai et al. 2003; Sakaida et al. 2004).

Analysis for the effect of recombinant FGF

Recombinant FGF1 (rFGF1) or rFGF2 (R&D Systems) was administered as follows. A treatment dose of 30 μ g/kg was deemed appropriate based on previous reports of clinical trials for ischemic heart diseases and peripheral vascular disorders (Laham et al. 2000; Lederman et al. 2002). C57 BL/6 female mice with CCl₄-induced chronic liver damage were divided into six groups: (1) CCl₄ group (treatment with neither BMCs nor rFGFs); (2) rFGF1 group (rFGF1-only treatment without BMT); (3) rFGF2 group (rFGF2-only treatment without BMT); (4) BMC group (BMC-only transplantation without rFGFs); (5) BMC+rFGF1 group (treatment with both BMCs and rFGF1); and (6) BMC+rFGF2 group (treatment with both BMCs and rFGF2). Isolated GFP-positive BMCs were incubated with rFGF1 or rFGF2 for approximately 30 s before transplantation and then injected into recipient mice with a 31-gauge needle and Hamilton syringe via the tail vein. After transplantation, CCl₄ injections were continued at the same dose twice a week. Mice were killed at 48 h after BMT and every week thereafter for up to 4 weeks. Immunohistochemical analysis with anti-GFP (Santa Cruz Biotechnology), anti-Liv2 (hepatoblast marker; Watanabe et al. 2002), anti-albumin (Bethyl Laboratories, Tex., USA), and anti-tumor necrosis factor- α (TNF- α ; TECHNE, Min., USA) antibodies was performed on these samples ($n=6$ in each group). The proportion of stained area was calculated by using MetaMorph software at a total of 30 random fields per group. Moreover, serum albumin level was measured ($n=6$ in each group) by using the SPOTCHEM EZ SP-4430 dry chemical system (Arkray, Kyoto, Japan; Terai et al. 2003; Sakaida et al. 2004). We calculated the survival rate with follow-up for 150 days after transplantation ($n=15$ in each group) by using the Kaplan-Meier method.

DNA-microarray analysis: first screen and second screen

We excised an equal amount of liver sample from three independent mice in each group at 48 h and 1 week after transplantation. Total RNA was isolated from the samples by using an Atlas Glass Total RNA Isolation Kit (Clontech, Palo Alto, Calif.), and single strands of cDNA were synthesized by using an Atlas Glass Fluorescent Labeling Kit (Clontech). DNA-microarray analysis was subsequently conducted with the Atlas Glass Mouse 1.0K Microarray System (Clontech; Omori et al. 2004; Ishigaki et al. 2002). The signal intensity of each gene was measured by a fluorescent scanner (Axon Instruments, Calif., USA), and the transient differences in gene expression between two groups were assessed with the Array Gauge System (Fuji Film, Tokyo, Japan). These methods were identical to those previously performed (Omori et al. 2004). In this study, a total of 1,108 genes on the DNA-microarray were analyzed, and two screens were carried out.

We did the first screen to select genes that were significantly up-regulated by BMT with rFGF2 treatment as compared with BMT-alone. For each gene, the gene expression was analyzed by the specific equations as follows:

x_{i1} ; expression level of gene i at 48 h after transplantation, in the BMC group

y_{i1} ; expression level of gene i at 48 h after transplantation, in BMC+rFGF2 group

x_{i2} ; expression level of gene i at 1 week after transplantation, in BMC group

y_{i2} ; expression level of gene i at 1 week after the transplantation in BMC+rFGF2 group

($i = 1, 2, 3, \dots, 1108$)

The chronological change of the expression level of gene i in each group was expressed as follows:

BMC group; $f_{i1} = \log_{10}(x_{i2}/x_{i1})$

BMC + rFGF2 group; $f_{i2} = \log_{10}(y_{i2}/y_{i1})$

The difference in the chronological change of the gene expression between two groups was defined by

$$F_i = f_{i2} - f_{i1} = \log_{10} \left[(y_{i2}/y_{i1}) / (x_{i2}/x_{i1}) \right]$$

If $(x_{i2}/x_{i1}) = (y_{i2}/y_{i1})$, the value of F_i , i.e., $\log_{10}1$ is zero. We focused on the genes with a large value of F .

For each gene, we computed the value of F and selected genes that fulfilled the conditions, $f_{i1} > 0$, $f_{i2} > 0$, and $F_i > 0.477 (= \log_{10}3)$. An $F_i > 0.477$ means that the ratio of y_{i2}/y_{i1} to x_{i2}/x_{i1} is more than 3. These genes were considered to be significantly up-regulated by rFGF2 treatment in addition to BMT.

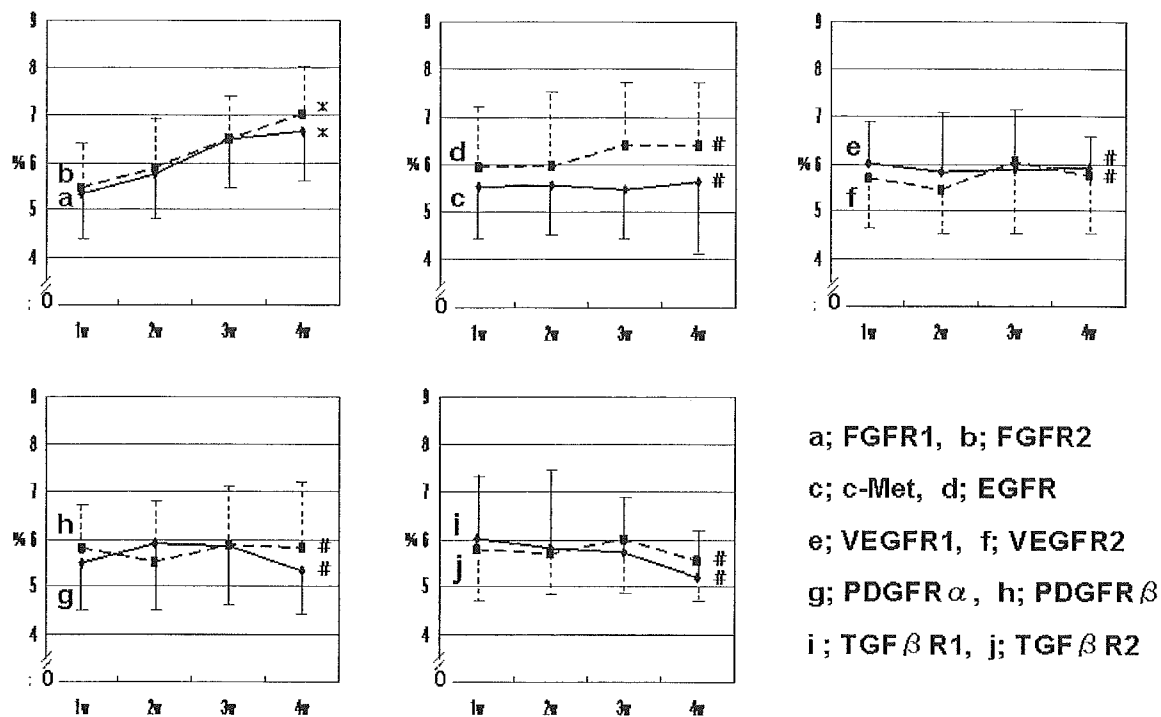


Fig. 1 Time-course of distribution of several growth factor receptors in the GFP/CCL₄ model system. Expression of FGFR1 and FGFR2 significantly increases with time after BMT (*x*-axis time after BMT (in weeks), *y*-axis percentage of stained area in immunohistochemistry).

*Significant difference compared with the value at 1 week ($P < 0.05$). #No significant difference compared with the value at 1 week ($P > 0.05$)

We carried out the second screen to separate the gene that was most specifically activated by rFGF2 treatment with BMT out of the genes selected from the screen I. This analysis was performed by using the additional equations as follows:

x'_{i1} ; expression level of gene *i* at 48 h in CCL₄ group
 y'_{i1} ; the expression level of gene *i* at 48 h in rFGF2 group
 x'_{i2} ; the expression level of gene *i* at 1 week in CCL₄ group

y'_{i2} ; the expression level of gene *i* at 1 week in rFGF2 group

$$\text{CCL}_4 \text{ group; } f_{i1} = \log_{10} (x'_{i2}/x'_{i1})$$

$$\text{rFGF2 group; } f_{i2} = \log_{10} (y'_{i2}/y'_{i1})$$

We compared the *f* value (chronological change of the gene expression) of each gene selected from screen I in two

Table 1 Percent immunohistochemically stained area in areas treated with anti-FGFR1 or anti-FGFR 2 and anti-FGF1 or anti-FGF2

Receptor or factor	Treatment	One week ^a	Four weeks ^b	Percentage change ^c
FGFR1	BMT(+) ^d	5.3%±1.0 ^e	6.7%±1.1 ^{e, f}	26.4%
	BMT(-) ^g	3.7%±0.7	4.2%±0.9	13.5%
FGFR2	BMT(+)	5.4%±0.9 ^e	7.0%±1.0 ^{e, f}	29.6%
	BMT(-)	3.8%±0.9	4.4%±1.0	15.8%
FGF1	BMT(+)	5.5%±0.9 ^e	7.1%±1.0 ^{e, f}	29.1%
	BMT(-)	3.8%±0.7	4.5%±0.5	18.4%
FGF2	BMT(+)	5.7%±1.1 ^e	7.5%±1.1 ^{e, f}	31.6%
	BMT(-)	3.9%±1.0	4.6%±1.0	17.9%

^aOne week in the BMT(-) group represents 5 weeks of CCL₄ injection

^bFour weeks in the BMT(-) group represents 8 weeks of CCL₄ injection

^cPercentage change over time (from 1 week to 4 weeks) in each group

^dBMT(+): BMC transplantation group with CCL₄-induced persistent liver damage

^eSignificant difference compared with the value at same period in the BMT(-) group ($P < 0.05$)

^fSignificant difference compared with the value at 1 week ($P < 0.05$)

^gBMT(-): control CCL₄-induced persistent liver damage group without BMT

BMT significantly elevates the expression of FGFRs and FGFs with time compared with the BMT (-) control group

Values are shown as means±SD

groups: the CCl₄ group and rFGF2 group. Those for the BMC group and BMC+rFGF2 group had been computed in screen I.

Western blot analysis of TNF- α

We isolated cell lysate from the liver sample at 1 week after transplantation in four groups: CCl₄ group, rFGF2 group, BMC group, and BMC+rFGF2 group. Protein was obtained by homogenization with lysis buffer (20 mM TRIS-HCl pH 7.5, 50 mM NaCl, 1 mM ethylenediaminetetraacetic acid, 1 mM ethyleneglycol-bis-N, N'-tetraacetic acid, 1% Triton X, 2.5 mM sodium pyrophosphate, 1 mM β -glycerophosphate,

1 mM Na₃VO₄, 1 μ g/ml leupeptin, and 1 mM phenylmethylsulfonyl fluoride) and then centrifuged. A total of 100 μ g protein were analyzed by sodium dodecylsulfate/polyacrylamide gel electrophoresis and immunoblot. Protein was electrophoretically transferred to a polyvinylidene difluoride membrane (Bio-Rad, CA, USA), which was incubated with a 1:500 dilution of goat anti-mouse TNF- α antibody, washed, and then incubated with a 1:5,000 dilution of anti-goat IgG conjugated to horseradish peroxidase (Amersham Biosciences, N.J., USA). Bands were visualized with an enhanced chemiluminescence Western blotting detection system (Amersham Biosciences, NJ, USA). All experiments were repeated independently at least three times with reproducible results.

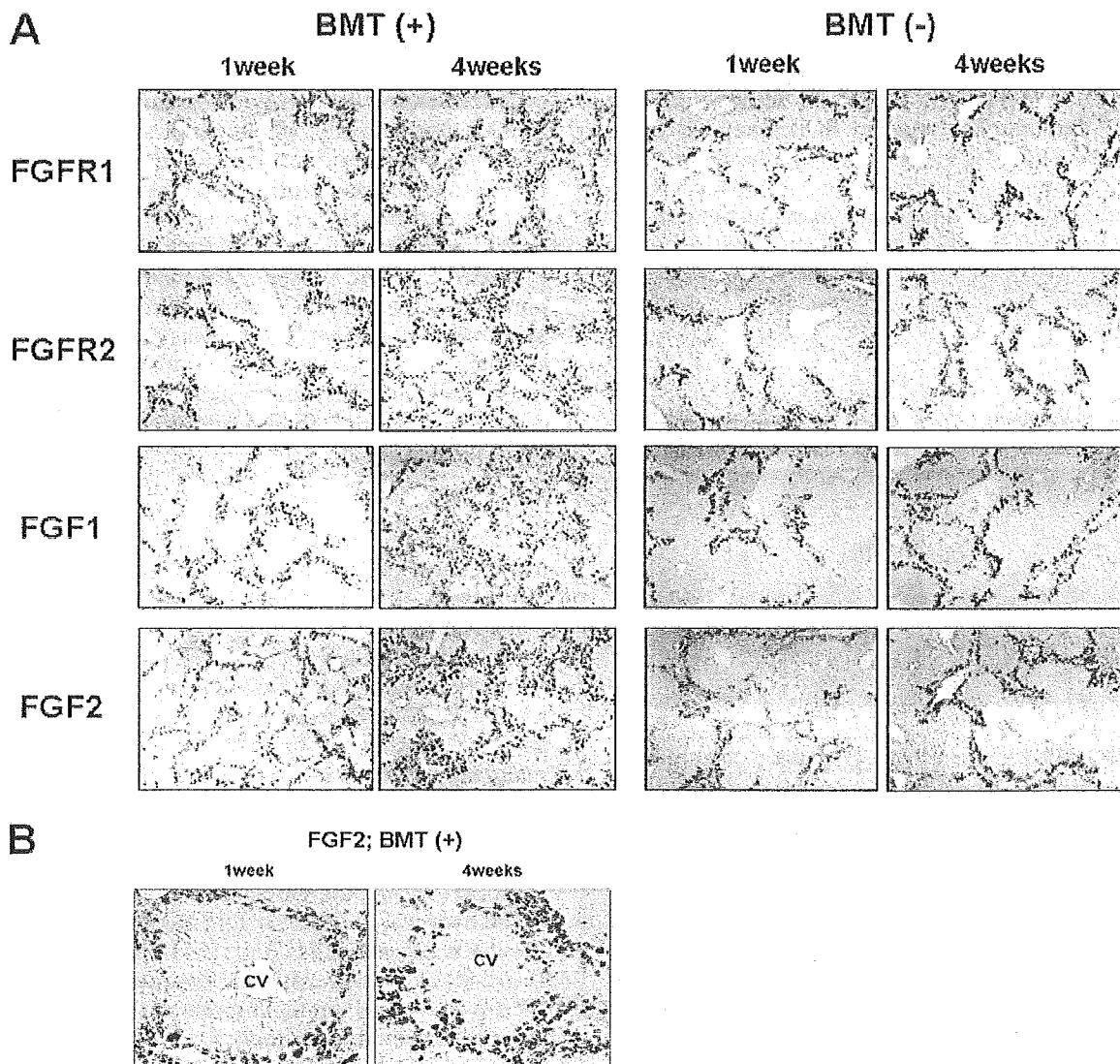


Fig. 2 Expression of FGFRs and FGFs (*BMT*(+) BMC transplantation group with CCl₄-induced persistent liver damage, *BMT*(-) control CCl₄-induced persistent liver damage group without BMC). One week (*1week*) in *BMT*(-) group represents 5 weeks of CCl₄ injection, and four weeks (*4weeks*) in *BMT*(-) group represents 8 weeks of CCl₄ injection. **A** Immunohistochemistry of FGFR1, FGFR2 and FGF1, FGF2 in *BMT*(+) and *BMT*(-) groups. In the

BMT(+) group, the expression of FGFRs and FGFs significantly increases with time as compared with the *BMT*(-) control group, and the distribution of the proteins eventually extends from the peri-portal area into the intra-lobule. $\times 40$ **B** Typical higher magnification image of FGF2 immunohistochemical staining in *BMT*(+) group. FGF2-positive cells proliferate and spread from the peri-portal area into the central area with time after BMT (*CV* central vein). $\times 200$

Statistical analysis

Values are shown as means±SD. Data were analyzed with Fisher's exact test. A *P*-value of <0.05 was considered statistically significant.

Results

Expression of FGFRs significantly increases with time after BMT

For screening, we performed immunohistochemical staining with ten different antibodies recognizing growth factor receptors in the GFP/CCL₄ model. As shown in Fig. 1a,b, the percentage of stained area for FGFR1 and FGFR2 gradually and significantly increased each week after BMT (*P*<0.05). On the other hand, the expression of other growth factor receptors (c-Met, EGFR, VEGFR1/2, PDGFR α/β, and TGFβR 1/2) could be detected, but no significant chronological change in the expression level after BMT was found (Fig. 1c–j). These results suggest that FGF-FGFR signaling is most closely related to the process of BMC differentiation into hepatocytes in our model.

Transplanted BMCs express FGFs and FGFRs during differentiation into hepatocytes

We further analyzed the expression of FGF1 and FGF2 and their receptors, FGFR1 and FGFR2, in the BMT(+) and BMT(–) groups. As shown in Table 1, BMT significantly elevated the percentage of the stained area of FGFRs and FGFs with time as compared with the BMT(–) control group (*P*<0.05). Furthermore, for each protein, the “percentage change” over time in the BMT(+) group was higher than that in the controls. Another obvious difference between the two groups was the distribution of the stained regions. Expression of FGFs and FGFRs was not detectable in the livers of normal mice (data not shown). In the BMT(–) group, expression of FGFs and FGFRs could be detected but consistently remained localized only to the peri-portal area. In contrast, in the BMT(+) group, expression of FGFs and FGFRs appeared to be up-regulated relative to control group, and the distribution of the proteins eventually extended from the peri-portal area into the intra-lobule (Fig. 2A). For example, the typical enlarged image of FGF2 immunohistochemical staining is shown in Fig. 2B. FGF2-positive cells proliferated and spread from the peri-portal area into the central area with time after BMT. To determine whether FGFs and FGFRs were detectable in the transplanted BMCs themselves, we analyzed the co-expression of GFP and FGFs or FGFRs. As shown in Fig. 3, co-expression of GFP and FGFRs was detectable at the cell surface. In addition, GFP and FGFs were both detected in the cytoplasm. These results indicate that transplanted BMCs express both FGFs and FGFRs during differentiation into hepatocytes.

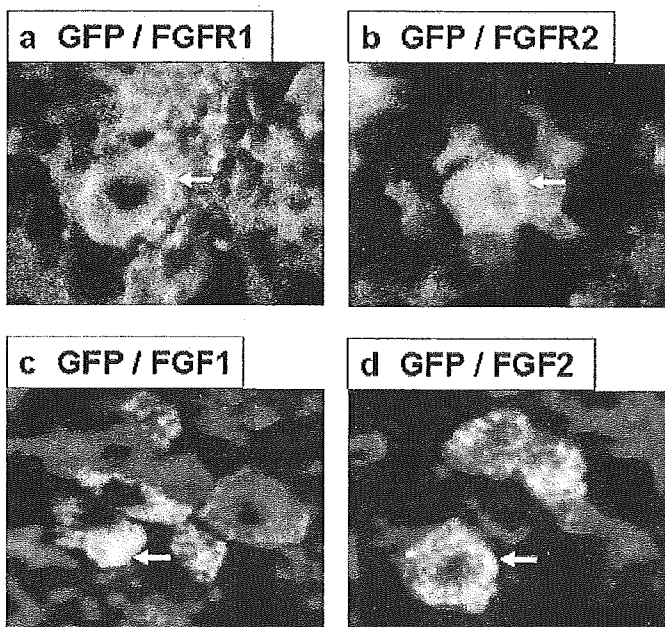


Fig. 3 Co-expression of GFP and FGFRs or FGFs in GFP/CCL₄ model. FGFRs are detectable at the cell surface of GFP-positive cells, and FGFs are detected in the cytoplasm of GFP-positive cells. Double-fluorescent merged images (arrows co-expression regions). **a** GFP (green), FGFR1 (red), co-expression of both GFP and FGFR1 (yellow). **b** GFP (green), FGFR2 (red), co-expression of both GFP and FGFR2 (yellow). **c** GFP (green), FGF1 (red), co-expression of both GFP and FGF1 (yellow). **d** GFP (green), FGF2 (red), co-expression of both GFP and FGF2 (yellow). ×400

FGF2 significantly elevates the repopulation rate of GFP-positive cells in the liver and increases the expression of both Liv2 and albumin

We investigated the effect of rFGF treatment on the process of the differentiation of BMCs into hepatocytes. In each group (BMC group, BMC+rFGF1 group, and BMC+rFGF2 group), the number of GFP-positive cells in the liver gradually increased after transplantation. GFP-positive cells were first detected in the peri-portal area and then in liver lobules with actively forming hepatic cords, suggesting a gradual spread into that region of the liver (Fig. 4A). In the BMC+rFGF1 group, the percentage of GFP-positive cells in the liver was 7.7±1.1% (1.4-fold more than in the BMC group) at 1 week, and 9.7±1.1% (1.2-fold more than in the BMC group) at 4 weeks after transplantation. The BMC+rFGF2 group showed the highest rate of liver repopulation among the three groups with a significant difference (*P*<0.05): 8.7±1.2% (1.6-fold more than in the BMC group, 1.1-fold more than in the BMC+rFGF1 group) at 1 week, and 10.7±1.2% (1.3-fold more than in the BMC group, 1.1-fold more than in the BMC+rFGF1 group) at 4 weeks after transplantation (Fig. 4B). The percentages of Liv2- and albumin-stained areas are summarized in Table 2. Treatment with rFGF, especially rFGF2, in combination with BMT

Fig. 4 Expression of GFP and Liv2 in BMC, BMC+rFGF1, and BMC+rFGF2 groups (BMC BMC-only transplantation without rFGF treatment BMC+rFGF1 treatment with both BMCs and rFGF1, BMC+rFGF2 treatment with both BMCs and rFGF2. **A** Immunohistochemistry for GFP.

GFP-positive cells in the liver gradually increase and spread from the peri-portal area into the intra-lobule with actively forming hepatic cords in each group. The level of GFP expression in the BMC+rFGF2 group is the highest amongst the three groups. $\times 200$. **B** Time-course of the percentage of GFP-positive cells in the liver. The BMC+rFGF2 group shows the highest percentage of stained area of GFP among three groups.

*Significant difference compared with the value at same period in BMC group ($P < 0.05$).

**Significant difference compared with the value at same period in BMC+rFGF1 group ($P < 0.05$).

C Immunohistochemistry for Liv2. The distribution of Liv2-positive cells in the liver is similar to that of GFP-positive cells, and the level of Liv2 expression in the BMC+rFGF2 group is the highest amongst the three groups. $\times 200$

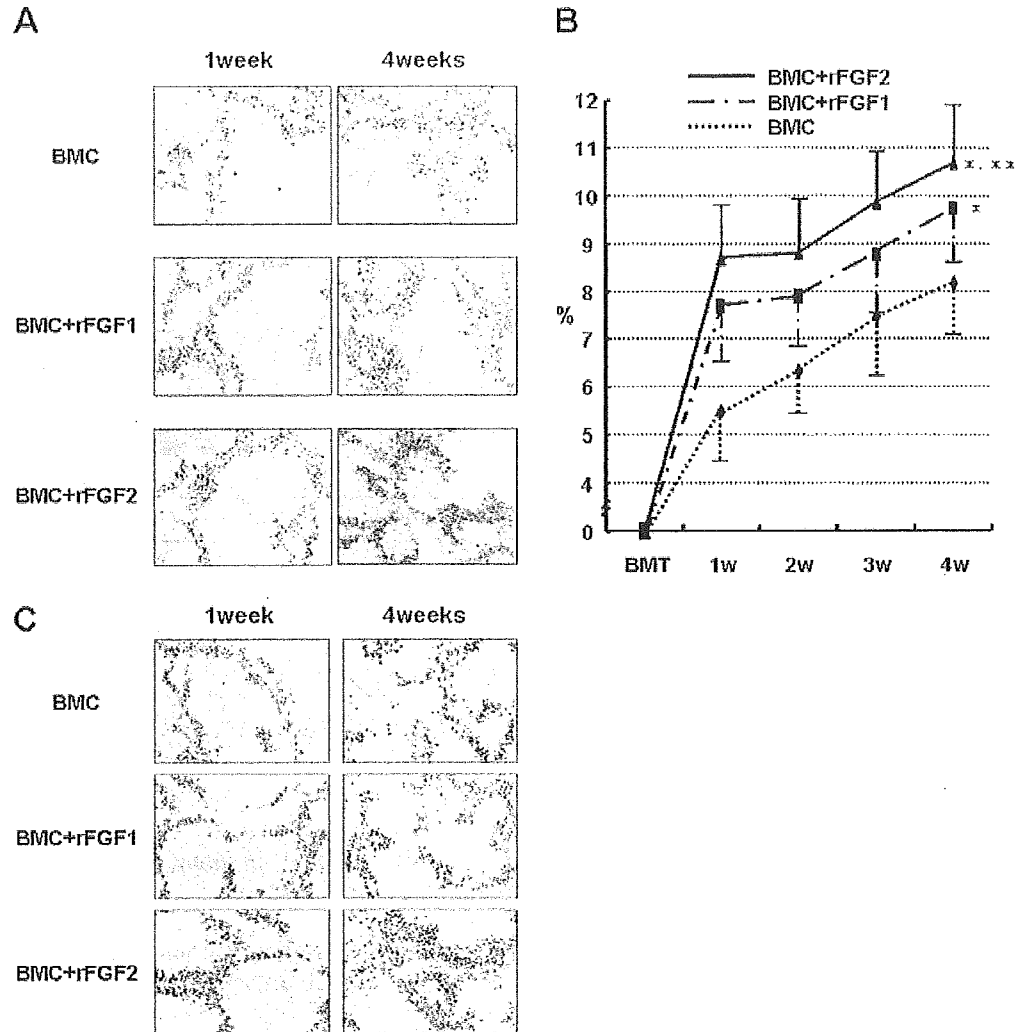


Table 2 Percentage area stained immunohistochemically for Liv2 and albumin

Protein	Treatment	One week	Four weeks
Liv2 (hepatoblast marker)	BMC ^a	5.4%±0.9	6.0%±0.7
	BMC+rFGF1 ^b	6.0%±0.6 ^c	6.8%±0.9 ^c
	BMC+rFGF2 ^d	6.3%±0.8 ^c	7.2%±0.9 ^{c, e}
Albumin (hepatocyte marker)	BMC	11.1%±1.0	12.1%±1.0
	BMC+rFGF1	11.9%±0.9 ^c	13.1%±1.0 ^c
	BMC+rFGF2	12.1%±0.8 ^c	13.6%±0.9 ^{c, e}

^aBMC BMC-only transplantation without rFGFs

^bBMC+rFGF1 Treatment with both BMCs and rFGF1

^cSignificant difference compared with the value at the same period in BMC group ($P < 0.05$)

^dBMC+rFGF2 Treatment with both BMCs and rFGF2

^eSignificant difference compared with the value at the same period in BMC+rFGF1 group ($P < 0.05$)

significantly increased the expression of both Liv2 and albumin compared with the BMC-only group ($P < 0.05$). Moreover, the distribution of Liv2-positive cells in the liver was similar to that of GFP-positive cells (Fig. 4C). On the other hand, we could not detect Liv2 expression in either the rFGF1 group or the rFGF2 group without BMT (data not shown). Thus, FGFs, especially FGF2, are likely, directly or indirectly, to facilitate the ability of transplanted BMCs to populate the liver and to differentiate into hepatocytes via hepatoblast intermediates.

Administration of rFGF2 in combination with BMT significantly elevates serum albumin level and survival rate of mice with damaged liver

Next, we focused on FGF2 and further analyzed the effect of rFGF2 treatment with BMT. We compared serum albumin levels and survival rates for four groups: CCl₄ group, rFGF2 group, BMC group, and BMC+rFGF2 group (Fig. 5A,B). BMT itself significantly elevated both values compared with those of the control CCl₄ group ($P < 0.05$), and BMT and rFGF2 treatment together resulted in serum albumin levels and survival rates that were significantly the

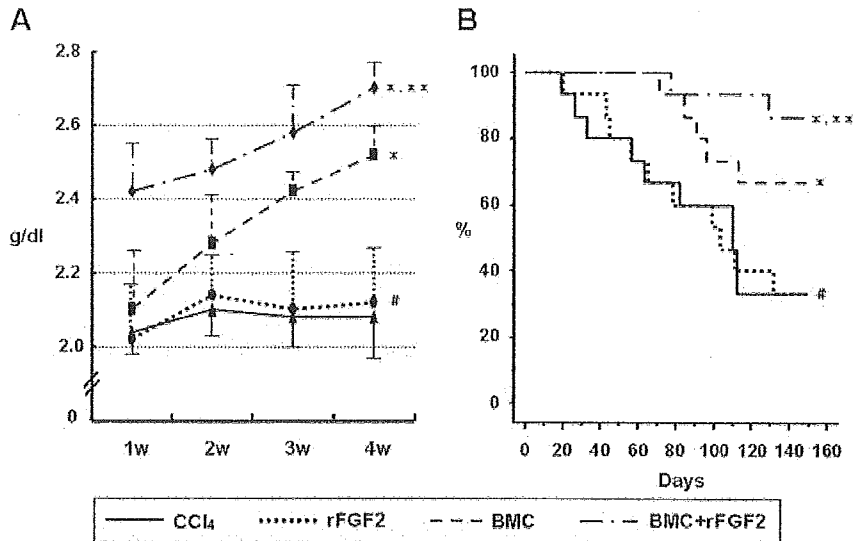


Fig. 5 Effect of rFGF2 treatment with BMT (CCl_4 treatment with neither BMCs nor rFGFs, $rFGF2$ rFGF2-only treatment without BMT, BMC BMC-only transplantation without rFGFs, $BMC+rFGF2$ treatment with both BMCs and rFGF2). **A** Time-course of serum albumin level. Serum albumin level is most significantly elevated by rFGF2 treatment in combination with BMT among four groups. *Significant difference compared with the value at the same period in the CCl_4 group ($P<0.05$). **Significant difference compared with the value at the same period in the BMC group

($P<0.05$). #No significant difference compared with the value at the same period in the CCl_4 group ($P>0.05$). **B** Cumulative survival analysis evaluated by the Kaplan-Meier method. Administration of rFGF2 with BMT improves the survival rate, which is significantly the highest among the four groups. *Significant difference compared with CCl_4 group ($P<0.05$). **Significant difference compared with BMC group ($P<0.05$). #No significant difference compared with CCl_4 group ($P>0.05$)

highest among the four groups ($P<0.05$). On the other hand, there was no significant difference between the CCl_4 group and rFGF2 group. These data suggest that administration of rFGF2 in combination with BMT is significantly the most effective for mice with damaged liver.

TNF- α signaling is activated by BMT with rFGF2 treatment

To improve our understanding of the molecular mechanism of the effect of FGF2 on the enhancement of the repop-

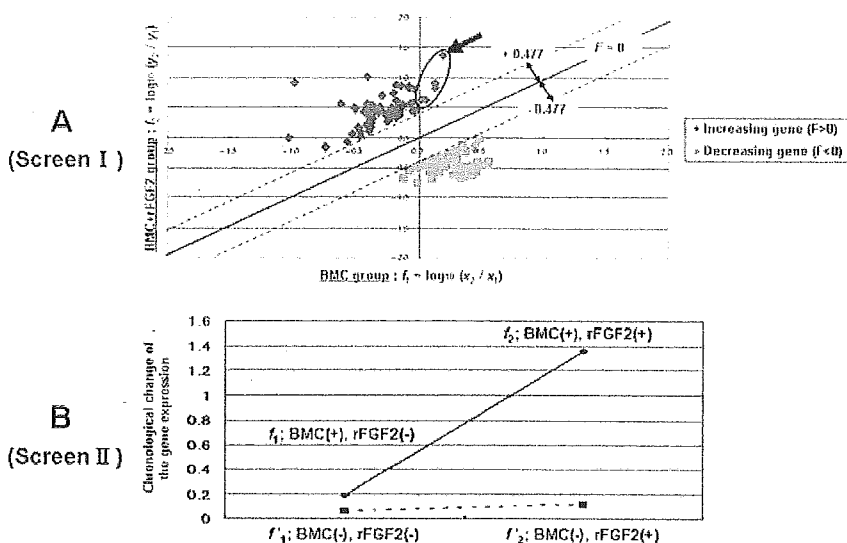


Fig. 6 Identification of the specific gene involved in repopulation and differentiation by using DNA-microarray analysis and two screens. **A** Plot of genes in the f_1 - f_2 space (Screen I). The five specific genes out of 1108 genes are selected in screen I (encircled plots the five selected genes, large arrow TNFIP3). **B** Chronological change of the gene expression of TNFIP3 (Screen II). TNFIP3 is most specifically activated by treatment with both BMCs and rFGF2 compared with

others in Screen II. The f value represents the chronological change of the expression level of a gene in each group (f_1 ; $BMC(-), rFGF2(-)$) CCl_4 group treated with neither BMCs nor rFGFs, f_2 ; $BMC(-), rFGF2(+)$ rFGF2-only treatment without BMT, f_3 ; $BMC(+), rFGF2(-)$ BMC-only transplantation without rFGFs, f_4 ; $BMC(+), rFGF2(+)$ treatment with both BMCs and rFGF2)

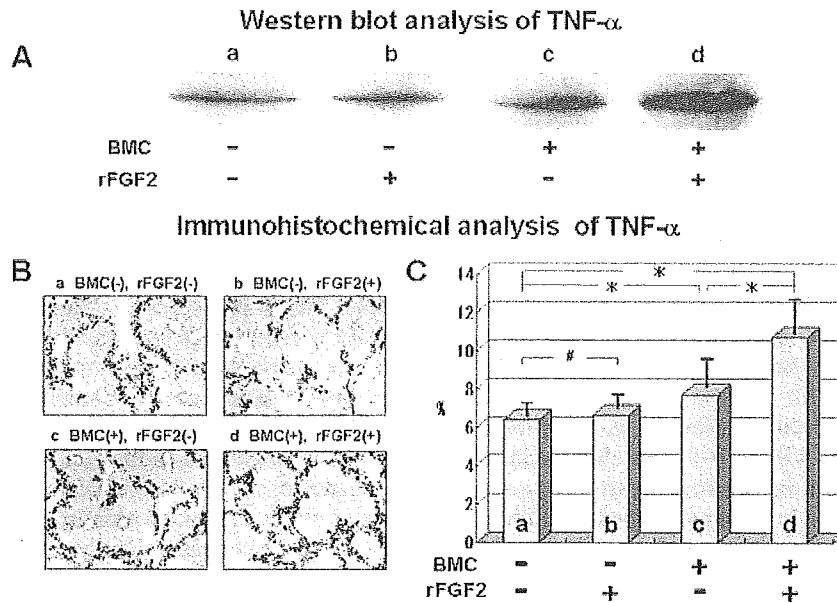


Fig. 7 Expression of TNF- α in CCl₄, rFGF2, BMC, and BMC+rFGF2 groups (a CCl₄ group: treatment with neither BMCs nor rFGFs, b rFGF2 group: rFGF2-only treatment without BMT, c BMC group: BMC-only transplantation without rFGFs, d BMC+rFGF2 group: treatment with both BMCs and rFGF2). A Western blot analysis of TNF- α . The level of TNF- α expression in BMC+rFGF2 group is the highest amongst the four groups in immunoblot analysis. B Immunohistochemical analysis of TNF- α . Expression of

TNF- α slightly increases with BMT-alone and is significantly elevated by rFGF2 treatment in combination with BMT compared with other treatments. $\times 40$ C Percentage of stained area of TNF- α . The BMC+rFGF2 group shows the highest percentage of stained area of TNF- α amongst the four groups. *Significant difference between two groups ($P < 0.05$). #No significant difference between two groups ($P > 0.05$)

ulation and differentiation of BMCs in the GFP/CCl₄ model, we used microarray analysis to profile the chronological change in gene expression before and after rFGF2 treatment. We carried out two screens to identify the specific gene that was activated by rFGF2 treatment in combination with BMT in mice with CCl₄-induced liver damage. Figure 6A shows the plot of genes in the 2-dimensional space spanned by f_1 and f_2 in screen I. We could select five genes that fulfilled the conditions $f_1 > 0$, $f_2 > 0$ and $F > 0.477$ ($= \log_{10} 3$), out of 1,108 genes. These specific genes are TNF- α induced protein 3 (TNFIP3), hypoxia-inducible factor 1 α , neural plakophilin-related arm-repeat protein, semaphorin B, and zinc-finger protein 46. Screen II was performed to separate the gene that was most specifically up-regulated by rFGF2 treatment with BMT out of five genes selected from screen I. In this analysis, TNFIP3 was most significantly activated when BMT and treatment with rFGF2 were combined compared with others (Fig. 6B). We next analyzed the expression of TNF- α protein in the liver from four groups at 1 week after transplantation: the CCl₄ group, rFGF2 group, BMC group, and BMC+rFGF2 group. Immunoblot analysis (Fig. 7A) revealed that BMT itself slightly elevated TNF- α expression, and the level of TNF- α expression in the BMC+rFGF2 group was the highest amongst the four groups. Immunohistochemical analysis confirmed the results of the immunoblot (Fig. 7B,C). Treatment of rFGF2 without BMT, by contrast, did not activate TNF- α signaling in our system. Together, these results suggest that

FGF2 significantly activates TNF- α signaling during the process of the differentiation of BMCs into hepatocytes.

Discussion

A number of reports have demonstrated the potential of BMCs to differentiate into a variety of cell types, including hepatocytes (Theise et al. 2000; Orlic et al. 2001; Ferrari et al. 1998; Lagasse et al. 2000; Krause et al. 2001; Kotton et al. 2001; Petersen et al. 1999; Okamoto et al. 2002). We have previously developed an in vivo model, the GFP/CCl₄ mouse model, and have reported that transplanted BMCs differentiate into albumin-producing functional mature hepatocytes via Liv2-positive immature hepatoblast intermediates (Terai et al. 2003). Furthermore, BMT elevates the serum albumin level, reduces liver fibrosis, and improves the survival rate in our model (Sakaida et al. 2004). The mechanism behind the BMC plasticity that we have observed in the model is the subject of much debate. For example, the mechanism could reportedly involve cell fusion, nuclear reprogramming, or trans-differentiation (Terada et al. 2002; Ying et al. 2002; Ianus et al. 2003; Hochedlinger et al. 2004; Harris et al. 2004; Jang et al. 2004), and several lines of evidence have led us to believe that both cell fusion and trans-differentiation might be important to BMC plasticity. We have previously performed microarray analysis (using specific equations with SOM) to analyze the molecular cues that controlled the differentiation of BMCs into hepatocytes in GFP/CCl₄

model and found a dramatic change of gene expression during BMC differentiation (Omori et al. 2004). In the early stage after BMT, genes known to regulate morphology, such as homeobox, helix-loop-helix transcription factors, and FGFs are up-regulated. In later stages, however, the genes that show relatively increased levels can be categorized as those associated with hepatocyte differentiation, such as hepatocyte nuclear factor-4 and glucose-6-phosphatase isomerase (Omori et al. 2004).

Several growth factors have previously been reported to play important roles in the repair processes in myocardium, vessel, nerve, skin, and bone (Detillieux et al. 2003; Kowalczyk and Pasyk 2002; Werner and Grose 2003; Goodman et al. 2003). Indeed, clinical trials of various growth factors (e.g., FGF, VEGF, HGF) for the treatment of peripheral vascular disorders, ischemic heart diseases, and cutaneous chronic wounds have been performed (Laham et al. 2000; Lederman et al. 2002; Fu et al. 2002). In this study, we have analyzed the expression of several growth factors and their receptors during the process of the repopulation and differentiation of BMCs into hepatocytes. We have found that the expression of FGFs and FGFRs significantly increases with time after BMT compared with other factors, and that the expression levels of FGFs and FGFRs are significantly higher in the BMT(+) group than in the BMT(-) control group ($P < 0.05$; Figs. 1, 2, Table 1). These results suggest that the FGF-FGFR system is important in our GFP/CCl₄ model. Furthermore, transplanted GFP-positive BMCs express both FGFs and FGFRs (Fig. 3). Our data indicate that transplanted BMCs differentiate into hepatocytes under the control of autocrine regulation by FGF signaling in the model system. These findings agree well with previous studies showing that FGF is crucial for the initial process of liver development (Kinoshita and Miyajima 2002; Jung et al. 1999; Deutsch et al. 2001). Indeed, a previous microarray-SOM analysis in our laboratory has demonstrated that FGF is an important factor at an early stage in the GFP/CCl₄ model (Omori et al. 2004). Taken together, these reports support our current finding that FGF-FGFR signaling plays important roles, especially during the early differentiation of BMCs into hepatocytes.

We have also investigated the way that the administration of rFGF affects the repopulation and differentiation of BMCs into hepatocytes in the GFP/CCl₄ model. Treatment with rFGF, especially rFGF2, significantly elevates the repopulation rate of GFP-positive cells in the liver and increases the expression of both Liv2 and albumin ($P < 0.05$; Fig. 4, Table 2). Furthermore, the serum albumin level is significantly elevated ($P < 0.05$; Fig. 5A), and the survival rate is significantly improved ($P < 0.05$; Fig. 5B) by treatment with rFGF2 in combination with BMT. In our present microarray analysis and screen I, we have been able to identify specific five genes that are significantly activated by BMT together with rFGF2 treatment compared with BMT-alone (Fig. 6A). In addition, as shown in Fig. 6B, screen II has revealed that TNFIP3 is most specifically up-regulated by rFGF2 treatment in combination with BMT amongst the five genes identified by screen

I. Interestingly, the induction of TNFIP3 (also called as A20) has been reported to be caused by TNF- α stimulation, and A20 is involved in feedback suppression of nuclear factor- κ B (NF- κ B) activation induced by TNF- α (Idel et al. 2003). We have not been able to obtain information regarding TNF- α expression itself, because our microarray system does not include it. We have lastly confirmed the expression of TNF- α protein during the differentiation of BMCs in GFP/CCl₄ model mice. BMT-alone slightly elevates TNF- α expression, and moreover, the level of TNF- α expression is significantly the highest when BMT and treatment with rFGF2 are combined, as shown by immunoblot and immunohistochemical analysis (Fig. 7). TNF- α is a pluripotent mediator that affects several cellular processes, including adhesion, migration, angiogenesis, and apoptosis. TNF- α -regulated inflammation signals, such as stress-activated protein kinase/extracellular signal regulated-kinase kinase 1/mitogen-activated protein-kinase kinase 4-mediated c-jun NH₂-terminal kinase signaling, are important for the generation of hepatoblasts (Watanabe et al. 2002). Yamada and Fausto (1998) have shown that the TNF receptor 1 signaling pathway involving NF- κ B, interleukin-6, and the signal transducer and activator of transcription 3, is an important component of the hepatocyte mitogenic response induced by CCl₄ injury in mouse liver. From these reports and our present studies, we speculate that the transplantation of BMCs and concurrent treatment with rFGF2 has a synergistic effect that facilitates or potentiates the differentiation of transplanted BMCs into hepatocytes through the activation of TNF- α signaling.

In conclusion, we have found that FGF2 is the most important growth factor in the GFP/CCl₄ model of liver damage and regenerative treatment. Our present studies suggest that FGF2 facilitates the differentiation of transplanted BMCs into albumin-producing hepatocytes via Liv2-positive hepatoblast intermediates through the activation of TNF- α signaling. Additionally, administration of FGF2 in combination with BMT improves the liver function and prognosis of mice with CCl₄-induced liver damage and might thus have the potential to become an effective and efficient therapy for patients with severe liver disease.

Acknowledgements We thank Dr. Masaru Okabe (Genome Research Center, Osaka University) for the gift of GFP transgenic mice and Mr. Jun Oba for valuable technical support.

References

- Alison MR, Poulosom R, Jeffery R, Dhillon AP, Quaglia A, Jacob J, Novelli M, Prentice G, Williamson J, Wright NA (2000) Hepatocytes from non-hepatic adult stem cells. *Nature* 406:257
- Detillieux KA, Sheikh F, Kardami E, Cattini PA (2003) Biological activities of fibroblast growth factor-2 in the adult myocardium. *Cardiovasc Res* 57:8-19
- Deutsch G, Jung J, Zheng M, Lora J, Zaret KS (2001) A bipotential precursor population for pancreas and liver within the embryonic endoderm. *Development* 128:871-881
- Ferrari G, Cusella-De Angelis G, Coletta M, Paolucci E, Stornaiuolo A, Cossu G, Mavilio F (1998) Muscle regeneration by bone marrow-derived myogenic progenitors. *Science* 279:1528-1530

- Fu X, Shen Z, Guo Z, Zhang M, Sheng Z (2002) Healing of chronic cutaneous wounds by topical treatment with basic fibroblast growth factor. *Chin Med J (Engl)* 115:331–335
- Goodman SB, Song Y, Yoo JY, Fox N, Trindade MC, Kajiyama G, Ma T, Regula D, Brown J, Smith RL (2003) Local infusion of FGF-2 enhances bone ingrowth in rabbit chambers in the presence of polyethylene particles. *J Biomed Mater Res* 65A:454–461
- Harris RG, Herzog EL, Bruscia EM, Grove JE, Van Arnam JS, Krause DS (2004) Lack of a fusion requirement for development of bone marrow-derived epithelia. *Science* 305:90–93
- Hochedlinger K, Blueloch R, Brennan C, Yamada Y, Kim M, Chin L, Jaenisch R (2004) Reprogramming of a melanoma genome by nuclear transplantation. *Genes Dev* 18:1875–1885
- Ianus A, Holz GG, Theise ND, Hussain MA (2003) In vivo derivation of glucose-competent pancreatic endocrine cells from bone marrow without evidence of cell fusion. *J Clin Invest* 111:843–850
- Idel S, Dansky HM, Breslow JL (2003) A20, a regulator of NFkappaB, maps to an atherosclerosis locus and differs between parental sensitive C57BL/6J and resistant FVB/N strains. *Proc Natl Acad Sci U S A* 100:14235–14240
- Ishigaki S, Niwa J, Ando Y, Yoshihara T, Sawada K, Doyu M, Yamamoto M, Kato K, Yotsumoto Y, Sobue G (2002) Differentially expressed genes in sporadic amyotrophic lateral sclerosis spinal cords—screening by molecular indexing and subsequent cDNA microarray analysis. *FEBS Lett* 531:354–358
- Jang YY, Collector MI, Baylin SB, Diehl AM, Sharkis SJ (2004) Hematopoietic stem cells convert into liver cells within days without fusion. *Nat Cell Biol* 6:532–539
- Jung J, Zheng M, Goldfarb M, Zaret KS (1999) Initiation of mammalian liver development from endoderm by fibroblast growth factors. *Science* 284:1998–2003
- Kinoshita T, Miyajima A (2002) Cytokine regulation of liver development. *Biochim Biophys Acta* 1592:303–312
- Kollet O, Shvitiel S, Chen YQ, Suriawinata J, Thung SN, Dabeva MD, Kahn J, Spiegel A, Dar A, Samira S, Goichberg P, Kalinkovich A, Arenzana-Seisdedos F, Nagler A, Hardan I, Revel M, Shafritz DA, Lapidot T (2003) HGF, SDF-1, and MMP-9 are involved in stress-induced human CD34+ stem cell recruitment to the liver. *J Clin Invest* 112:160–169
- Kotton DN, Ma BY, Cardoso WV, Sanderson EA, Summer RS, Williams MC, Fine A (2001) Bone marrow-derived cells as progenitors of lung alveolar epithelium. *Development* 128:5181–5188
- Kowalczyk J, Pasyk S (2002) Vascular endothelial growth factor and its application in therapy of cardiovascular diseases. *Pol Merkuriusz Lek* 13:74–78
- Krause DS, Theise ND, Collector MI, Henegariu O, Hwang S, Gardner R, Neutzel S, Sharkis SJ (2001) Multi-organ, multi-lineage engraftment by a single bone marrow-derived stem cell. *Cell* 105:369–377
- Lagasse E, Connors H, Al-Dhalimy M, Reitsma M, Dohse M, Osborne L, Wang X, Finegold M, Weissman IL, Grompe M (2000) Purified hematopoietic stem cells can differentiate into hepatocytes in vivo. *Nat Med* 6:1229–1234
- Laham RJ, Chronos NA, Pike M, Leimbach ME, Udelson JE, Pearlman JD, Pettigrew RI, Whitehouse MJ, Yoshizawa C, Simons M (2000) Intracoronary basic fibroblast growth factor (FGF-2) in patients with severe ischemic heart disease: results of a phase I open-label dose escalation study. *J Am Coll Cardiol* 36:2132–2139
- Lederman RJ, Mendelsohn FO, Anderson RD, Saucedo JF, Tenaglia AN, Hermler JB, Hillegeass WB, Roccha-Singh K, Moon TE, Whitehouse MJ, Annex BH (2002) Therapeutic angiogenesis with recombinant fibroblast growth factor-2 for intermittent claudication (the TRAFFIC study): a randomised trial. *Lancet* 359:2053–2058
- Okamoto R, Yajima T, Yamazaki M, Kanai T, Mukai M, Okamoto S, Ikeda Y, Hibi T, Inazawa J, Watanabe M (2002) Damaged epithelia regenerated by bone marrow-derived cells in the human gastrointestinal tract. *Nat Med* 8:1011–1017
- Omori K, Terai S, Ishikawa T, Aoyama K, Sakaida I, Nishina H, Shinoda K, Uchimura S, Hamamoto Y, Okita K (2004) Molecular signature associated with plasticity of bone marrow cell under persistent liver damage by self-organizing-map-based gene expression. *FEBS Lett* 578:10–20
- Orlic D, Kajstura J, Chimenti S, Jakoniuk I, Anderson SM, Li B, Pickel J, McKay R, Nadal-Ginard B, Bodine DM, Leri A, Anversa P (2001) Bone marrow cells regenerate infarcted myocardium. *Nature* 410:701–705
- Petersen BE, Bowen WC, Patrene KD, Mars WM, Sullivan AK, Murase N, Boggs SS, Greenberger JS, Goff JP (1999) Bone marrow as a potential source of hepatic oval cells. *Science* 284:1168–1170
- Sakaida I, Terai S, Yamamoto N, Aoyama K, Ishikawa T, Nishina H, Okita K (2004) Transplantation of bone marrow cells reduces CCl4-induced liver fibrosis in mice. *Hepatology* 40:1304–1311
- Shinoda K, Mori S, Ohtsuki T, Osawa Y (1992) An aromatase-associated cytoplasmic inclusion, the “stigmoid body,” in the rat brain. I. Distribution in the forebrain. *J Comp Neurol* 322:360–376
- Stamm C, Westphal B, Kleine HD, Petzsch M, Kittner C, Klinge H, Schumichen C, Nienaber CA, Freund M, Steinhoff G (2003) Autologous bone-marrow stem-cell transplantation for myocardial regeneration. *Lancet* 361:45–46
- Terada N, Hamazaki T, Oka M, Hoki M, Mastalerz DM, Nakano Y, Meyer EM, Morel L, Petersen BE, Scott EW (2002) Bone marrow cells adopt the phenotype of other cells by spontaneous cell fusion. *Nature* 416:542–545
- Terai S, Sakaida I, Yamamoto N, Omori K, Watanabe T, Ohata S, Katada T, Miyamoto K, Shinoda K, Nishina H, Okita K (2003) An in vivo model for monitoring trans-differentiation of bone marrow cells into functional hepatocytes. *J Biochem (Tokyo)* 134:551–558
- Theise ND, Nimmakayalu M, Gardner R, Illei PB, Morgan G, Teperman L, Henegariu O, Krause DS (2000) Liver from bone marrow in humans. *Hepatology* 32:11–16
- Wang X, Ge S, McNamara G, Hao QL, Crooks GM, Nolte JA (2003) Albumin-expressing hepatocyte-like cells develop in the livers of immune-deficient mice that received transplants of highly purified human hematopoietic stem cells. *Blood* 101:4201–4208
- Watanabe T, Nakagawa K, Ohata S, Kitagawa D, Nishitai G, Seo J, Tanemura S, Shimizu N, Kishimoto H, Wada T, Aoki J, Arai H, Iwatsubo T, Mochizuki M, Satake M, Ito Y, Matsuyama T, Mak T, Penninger J, Nishina H, Katada T (2002) SEK1/MKK4-mediated SAPK/JNK signaling participates in embryonic hepatoblast proliferation via a pathway different from NF-kappaB-induced anti-apoptosis. *Dev Biol* 250:332–347
- Werner S, Grose R (2003) Regulation of wound healing by growth factors and cytokines. *Physiol Rev* 83:835–870
- Wexler SA, Donaldson C, Denning-Kendall P, Rice C, Bradley B, Hows JM (2003) Adult bone marrow is a rich source of human mesenchymal “stem” cells but umbilical cord and mobilized adult blood are not. *Br J Haematol* 121:368–374
- Yamada Y, Fausto N (1998) Deficient liver regeneration after carbon tetrachloride injury in mice lacking type 1 but not type 2 tumor necrosis factor receptor. *Am J Pathol* 152:1577–1589
- Yamamoto N, Terai S, Ohata S, Watanabe T, Omori K, Shinoda K, Miyamoto K, Katada T, Sakaida I, Nishina H, Okita K (2004) A subpopulation of bone marrow cells depleted by a novel antibody, anti-Liv8, is useful for cell therapy to repair damaged liver. *Biochem Biophys Res Commun* 313:1110–1118
- Ying QL, Nichols J, Evans EP, Smith AG (2002) Changing potency by spontaneous fusion. *Nature* 416:545–548

Lesson from the GFP/CCl₄ model — Translational Research Project: the development of cell therapy using autologous bone marrow cells in patients with liver cirrhosis

SHUJI TERAI¹, ISAO SAKAIDA¹, HIROSHI NISHINA², and KIWAMU OKITA¹

¹Department of Molecular Science and Applied Medicine (Gastroenterology and Hepatology), Yamaguchi University School of Medicine, 1-1-1 Minami Kogushi, Ube, Yamaguchi 755-8505, Japan

²Department of Developmental and Regenerative Biology, Medical Research Institute, Tokyo Medical and Dental University, Tokyo, Japan

Abstract

The plasticity of bone marrow has been confirmed by the analysis of autopsy findings in female recipients of bone marrow cells transplanted from male donors. To establish new clinical cell therapies using autologous bone marrow cells for patients with liver failure, we developed a new *in vivo* model, the “green fluorescent protein (GFP)/carbon tetrachloride (CCl₄) model”. Using the GFP/CCl₄ model, we found that transplanted Liv8-negative cells efficiently repopulated into cirrhotic liver tissue and trans-differentiated into albumin-producing hepatocytes under conditions of persistent liver damage induced by CCl₄. Moreover, one marrow cell transplantation into liver cirrhosis mice improved their liver function, ameliorated liver fibrosis, and improved their survival rate. Results from the GFP/CCl₄ model showed that cell therapy using autologous bone marrow cells has the potential to become an effective treatment for patients with liver failure. Here we describe the findings from the GFP/CCl₄ model and the scope of the translational research project.

Key words Bone marrow cells · Bone marrow cell transplantation · Liver cirrhosis · GFP (green fluorescent protein)/carbon tetrachloride (CCl₄) model · Liver fibrosis · Stem cell · Translational research · Trans-differentiation · Niche · Liver fibrosis

Introduction

Liver failure in patients with liver cirrhosis with endstage chronic liver disease is very difficult to cure. At present, liver transplantation is one effective therapy for curing these patients; however, this treatment faces serious problems, such as lack of donors, operative damage, rejection, and high expense. On the other hand, cell transplantation therapy is a minimally invasive procedure with fewer potential complications. Regenerative medicine using stem cells is an attractive

therapy for the cure of patients with severe liver disease. The capacity of bone marrow cells (BMCs) to differentiate into hepatocytes and intestinal cells was confirmed through the detection of the Y chromosome in the analysis of autopsy findings in human female recipients of BMCs from male donors.^{1–4} BMCs are an attractive cell source for regenerative medicine, because it is easier to obtain BMCs than it is to obtain other tissue-specific stem cells.^{5,6} BMC transplantation is also an established treatment for hematological diseases. Clinical studies have evaluated the use of BMCs in regenerating the myocardium and vessels in patients with heart failure and those with limb ischemia.^{7–10} Based on these findings, we began to focus on BMCs as a new cell source for liver regenerative therapy. The mechanism of BMC plasticity was previously examined with respect to cell fusion^{11,12} and trans-differentiation.^{13,14} We think that the most important aspect of developing a new clinical therapy using BMCs is evaluating its effectiveness for liver disease. We think both cell fusion and trans-differentiation could be important for furthering the understanding of the mechanisms of BMC plasticity. Indeed, the development of an effective cell therapy using BMCs requires better understanding of events in the recipient mouse liver after BMC transplantation. We developed a new *in vivo* model, named the “green fluorescent protein (GFP)/carbon tetrachloride (CCl₄) model”,¹⁵ in which to monitor the differentiation of BMCs into functional hepatocytes. Here, we describe the newest findings from the GFP/CCl₄ model. These lessons will be important for proceeding with the translational project of cell therapy using autologous BMCs to treat patients with liver cirrhosis.

The GFP/CCl₄ model

First, we sought to understand how to use BMCs to repair liver damage, using our GFP/CCl₄ model.¹⁵ In the

Offprint requests to: S. Terai

Received: February 14, 2005 / Accepted: February 28, 2005